

**DESIGN AND PERFORMANCE EVALUATION OF TRANS-
RECEIVE SCHEMES FOR OFDM WITH INDEX
MODULATION**

BY

MOHAMMAD UMAIR YAQUB

A Thesis Presented to the
DEANSHIP OF GRADUATE STUDIES

KING FAHD UNIVERSITY OF PETROLEUM & MINERALS

DHAHRAN, SAUDI ARABIA

In Partial Fulfillment of the
Requirements for the Degree of

MASTER OF SCIENCE

In

TELECOMMUNICATION ENGINEERING

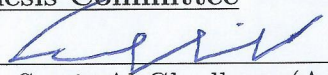
MAY 2016

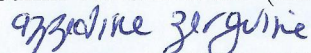
KING FAHD UNIVERSITY OF PETROLEUM & MINERALS
DHAHRAN 31261, SAUDI ARABIA

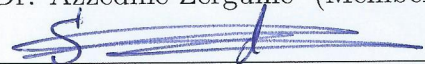
DEANSHIP OF GRADUATE STUDIES

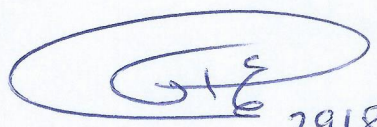
This thesis, written by **MOHAMMAD UMAIR YAQUB** under the direction of his thesis advisor and approved by his thesis committee, has been presented to and accepted by the Dean of Graduate Studies, in partial fulfillment of the requirements for the degree of **MASTER OF SCIENCE IN TELECOMMUNICATION ENGINEERING**.

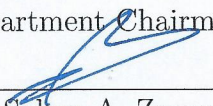
Thesis Committee


Dr. Samir Al-Ghadban (Advisor)

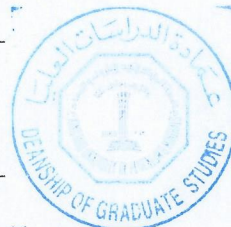

Dr. Azzedine Zerguine (Member)


Dr. Saad Al-Ahmadi (Member)


Dr. Ali Al-Shaikhi
Department Chairman


Dr. Salam A. Zummo
Dean of Graduate Studies


Date



©Mohammad Umair Yaqub
2016

Dedication

*I dedicate this to my mother, family and medieval Muslim
scientists.*

ACKNOWLEDGMENTS

First of all, I am grateful to Allah for raising me in such a great academic environment where I was able to pursue my higher education in a loving and peaceful atmosphere. I would like to send my blessings to our beloved Prophet Mohammad (PBUH) who was the best teacher and whom we follow and look towards for inspiration.

*I am extremely grateful to **Dr. Samir Al-Ghadhban** for taking me on as his student and giving me the opportunity to do my research with him. I would like to express my gratitude for his constant moral and academic support. I also valued his advice, ideas and suggestions without all of which, this thesis would not have been possible. Most of all, I am extremely thankful for his consistent guidance throughout this period and for being on my side through thick and thin.*

*I also would like to thank my thesis committee members **Dr. Saad Al-Ahmadi** and **Dr. Azzedine Zerguine** who have provided constant support and motivation. Dr. Al-Ahmadi has shown a great interest in my progress and allowed me to be part of the MIMO USRIP training event. Dr. Zerguine has always been ready with a kind word of and has encouraged me to do my best.*

*I also express my gratitude to the **Deanship of Graduate Studies** especially **Dr. Salam Zummo** and the **Electrical Engineering Department** who al-*

lowed me to pursue my graduate studies as a Research Assistant. This position allowed me to gain valuable teaching experience in addition to my degree and research.

I would like to thank **KFUPM** as an institution especially the rector **Dr. Khalid Al-Sultan** for giving the sons of faculty members the opportunity to pursue their degrees. In addition to them, I acknowledge the roles of the **Ministry of Higher Education** and the **Government of Saudi Arabia**. Due to their generosity and hospitality, hopefully I will graduate and obtain a Master's degree in the coming days from the same institution as my father.

On that subject, I thank my **father** for his constant encouragement to obtain the highest degree possible. More importantly, I would like to emphatically acknowledge the role my **mother** has played throughout this process. She has basically been a life manager who has enabled me to pursue my goals and dreams. I would like to thank my brothers for their love and support as well along with my extended family.

Lastly, I take this opportunity to appreciate the wider **KFUPM community**. Most of these people have seen me grow from a little child to the man I am today.

TABLE OF CONTENTS

ACKNOWLEDGEMENTS	iii
LIST OF TABLES	viii
LIST OF FIGURES	ix
NOMENCLATURE	xi
ABSTRACT (ENGLISH)	xv
ABSTRACT (ARABIC)	xvii
CHAPTER 1 INTRODUCTION	1
1.1 Introduction to wireless communications	2
1.2 Orthogonal Frequency Division Multiplexing (OFDM)	3
1.2.1 OFDM with Index Modulation (OFDM-IM)	4
1.3 Thesis Scope and Motivation	4
1.4 Thesis Contributions	6
1.5 Thesis Organization	7
1.5.1 Important Notations	8
CHAPTER 2 BACKGROUND AND LITERATURE REVIEW	10
2.1 OFDM	10
2.2 Narrow-band Interference	12
2.3 MIMO	13

2.4	Spatial Modulation	14
2.4.1	SM Review	15
2.4.2	SSK Review	16
2.4.3	SM-OFDM	17
2.5	OFDM-IM	17
2.5.1	Sub-Carrier Index Modulation	18
2.5.2	OFDM with Index Modulation	20
2.6	MIMO-OFDM-IM	22
2.7	Generalized OFDM-IM	23
2.8	Interleaved OFDM-IM	24
2.9	OFDM-IM Evaluation	25
2.10	OFDM-IM for Visible Light Communication (VLC)	27
2.11	Summary	27
CHAPTER 3 REVIEW OF OFDM-IM		28
3.1	OFDM-IM System Model	28
3.2	Look-Up Table Implementation	31
3.3	ML Receiver implementation	33
3.3.1	ML Receiver Architecture	35
3.4	OFDM-IM Performance	35
3.5	Summary	37
CHAPTER 4 OFDM WITH INDEX SHIFT KEYING		38
4.1	OFDM-GISK	39
4.1.1	System Design	39
4.1.2	ML Receiver implementation	42
4.2	OFDM-ISK	44
4.2.1	System Design	44
4.2.2	ML Receiver implementation	45
4.3	Performance Evaluation of OFDM-GISK	47
4.3.1	Extension to OFDM-ISK	53

4.4	Results and Discussion	54
4.5	Summary	58
CHAPTER 5 INTERFERENCE: EFFECTS AND MITIGATION		59
5.1	NBI impairment in OFDM-IM	60
5.1.1	NBI Signal Model	61
5.2	Mitigation using compressed sensing	62
5.2.1	Compressed Sensing introduction	63
5.2.2	OFDM-IM with zero padding	64
5.2.3	Zero Forcing matrix	65
5.2.4	Modified CS based approach	66
5.3	NBI simulation results and analysis	68
5.3.1	Impact of jammer width w	69
5.3.2	Impact of Interference Power	70
5.3.3	Performance degradation in OFDM-IM	74
5.3.4	NBI Mitigation Results	74
5.4	Review of ICI in OFDM-IM	77
5.4.1	Signal Model	78
5.4.2	ICI cancellation schemes for OFDM-IM	79
5.4.3	Performance of various ICI cancellation schemes for OFDM- IM	81
5.5	Performance of ISK techniques in the presence of ICI	83
5.6	Summary	85
CHAPTER 6 CONCLUSION		86
6.1	Conclusions	86
6.2	Future Research	88
REFERENCES		89
VITAE		99

LIST OF TABLES

3.1	An example of index selection for $n = 4$ and $k = 2$	32
3.2	OFDM-IM parameters for $N = 16$ carriers with $n = 4$, $k = 2$ and $M = 4$	32
3.3	Examples of sub-blocks generated for the system and input bits described by Table 3.1 and look-up table described by Table 3.2 .	33

LIST OF FIGURES

2.1	Illustration of the work done on OFDM-IM in literature	18
3.1	Block Diagram of the OFDM-IM block generator	31
3.2	BER versus E_b/N_o for OFDM-IM for $n = 4$ and $k = 2$ using QPSK	36
3.3	Comparison of the BER versus E_b/N_o for OFDM-IM for $n = 4$ and $k = 2$ using BPSK and QPSK	37
4.1	Block Diagram of an OFDM-GISK transmission.	41
4.2	Block Diagram of an OFDM-ISK transmission.	45
4.3	BER versus E_b/N_o OFDM-ISK for various values of N	55
4.4	BER versus E_b/N_o OFDM-GISK for $N = 8$ and $n = 1, \dots, 7$. . .	56
4.5	Simulation and theoretical results for OFDM-GISK for $N = 8$ and $n = 1, \dots, 4$	57
4.6	Simulation and theoretical results for OFDM-GISK for $N = 8$ and $n = 1, \dots, 4$	57
4.7	Comparison of OFDM-GISK with $N = 8$ and $n = 1$ and 3 versus OFDM-IM.	58
5.1	BER versus w for OFDM and OFDM-IM for $E_b/N_o = 15dB$. . .	70
5.2	BER versus w for OFDM and OFDM-IM for $E_b/N_o = 15dB$. . .	71
5.3	BER versus SNIR of OFDM and OFDM-IM in presence of 1 and 3 jammers at an SNR of 15dB.	72
5.4	BER versus SNIR of OFDM and OFDM-IM in presence of 1 and 3 jammers at an SNR of 20dB.	73

5.5	BER versus SNIR of OFDM and OFDM-IM in presence of one and three jammers at an SNR's of 15 and 20 dB.	73
5.6	Performance of OFDM and OFDM-IM in presence of one jammer.	75
5.7	Performance of OFDM and OFDM-IM in presence of three jammers.	75
5.8	Performance of OFDM and OFDM-IM in presence of 3 jammers .	76
5.9	Performance of OFDM-IM in presence of 3 jammers after cancellation for an SNIR of -15dB	77
5.10	Performance of various ICI cancellation schemes of OFDM-IM at 100km/h.	82
5.11	Performance of various ICI cancellation schemes of OFDM-IM at 300 km/h.	83
5.12	Performance of OFDM-GISK for $N = 8$ at 100 km/h.	84
5.13	Performance of OFDM-GISK for $N = 16$ at 100 km/h.	85

NOMENCLATURE

Symbol	Description
4G	Fourth generation networks
5G	Fifth generation networks
AE	Antenna Element
BC	Block Cancellation
BPSK	Binary Phase Shift Keying
CS	Compressive Sensing
CSI	Channel State Information
DFT	Discrete Fourier Transform
EE	Energy Efficiency
ESIM	Enhanced Sub-Carrier Index Modulation
FFT	Fast Fourier Transform
GPSSK	Generalized Phase Space Shift Keying
GSSK	Generalized Space Shift Keying
ICI	Inter-Carrier Interference
IEEE	Institute of Electrical and Electronics Engineers
IFFT	Inverse Fast Fourier Transform
IM	Index Modulation

ISK	Index Shift Keying
LLR	Log Likelihood Ratio
LTE	Long-Term Evolution
MAE	Multiple Antenna Element
MIMO	Multiple-Input Multiple-Output
MISO	Multiple-Input Single-Output
MMSE	Minimum Mean Square Error
NBI	Narrowband Interference
OFDM	Orthogonal Frequency Division Multiplexing
OFDM-GIM	OFDM with Generalized Index Modulation
OFDM-GISK	Orthogonal Frequency Division Multiplexing with Generalized Index Shift Keying
OFDM-I/Q-IM	OFDM with In-phase/Quadrature Index Modu- lation
OFDM-IM	Orthogonal Frequency Division Multiplexing with Index Modulation
OFDM-ISIM	OFDM with Interleaved Subcarrier Index Modu- lation
OFDM-ISK	Orthogonal Frequency Division Multiplexing with Index Shift Keying
PSK	Phase Shift Keying
QAM	Quadrature Amplitude Modulation

QPSK	Quadrature Phase Shift Keying
RF	Radio Frequency
RFC	Radio Frequency Chain
SCIR	Signal-to-inter-Carrier Interference Ratio
SE	Spectral Efficiency
SIM	Sub-Carrier Index Modulation
SIMO	Single-Input Multiple-Output
SM	Spatial Modulation
SP	Signal Power
SSK	Space Shift Keying
\det	Determinant of a Matrix
RV	Random Variable
pdf	Probability density function
i.i.d	independent and identically distributed
\mathcal{CN}	Circularly-symmetric complex normal
$\mathbb{C}^{N \times M}$	Complex $N \times M$ matrix
$\mathbb{R}^{N \times M}$	Real $N \times M$ matrix
A	Matrix
I_N	$N \times N$ Identity Matrix
\mathcal{F}	Fourier Transform
\mathcal{F}^{-1}	Inverse Fourier Transform
a	Column vector

\mathbf{a}_i	Vector indexed for some purpose
a_i	The i .th element of the vector \mathbf{a}
a	Scalar
$\text{tr} ()$	Trace of a Matrix
$ \cdot $	l -1 norm
$\ \cdot\ $	l -2 norm
$\ \cdot\ _F$	Frobenius norm

THESIS ABSTRACT

NAME: MOHAMMAD UMAIR YAQUB

TITLE OF STUDY: DESIGN AND PERFORMANCE EVALUATION OF
TRANS-RECEIVE SCHEMES FOR OFDM WITH IN-
DEX MODULATION

MAJOR FIELD: TELECOMMUNICATION ENGINEERING

DATE OF DEGREE: MAY 2016

The demand for wireless technologies that provide high data rates and performance is ever increasing. With the advent of new wireless technologies such as 5G and vehicular networks and the shift towards large scale cooperative Multiple Input Multiple Output (MIMO), it is imperative that the resources are utilized optimally. Orthogonal Frequency Division Multiplexing (OFDM) is a promising and widely used technique in wireless communications. Recently, a new family of schemes called OFDM with Index Modulation (OFDM-IM) based on the concept of Spatial Modulation (SM) have been proposed. OFDM-IM provides better performance in wireless channels and is more resilient to interference. In this thesis, a new family of OFDM-IM techniques called OFDM with Index Shift Keying

(OFDM-ISK) are designed and the impact of Narrowband Interference (NBI) on OFDM-IM is studied. It is shown analytically and by simulations that the newly designed schemes perform better than OFDM-IM. In addition, OFDM-IM is evaluated under (NBI) and simulations illustrate that unlike classical OFDM, IM can withstand the effects of NBI to a greater degree. A mitigation technique is proposed and implemented to improve the performance at very high interference. Lastly, the newly designed techniques are studied under ICI to examine the trade-off between the number of active sub-carriers and performance.

الاسم الكامل: محمد عمير يعقوب

عنوان الرسالة: تصميم وتقييم أداء مخططات ارسال واستقبال لتردد المتعامد بالتقسيم (OFDM) مع تعديل الرقم التسلسلي

التخصص: هندسة الاتصالات

تاريخ الدرجة العلمية: مايو، ٢٠١٦م

الطلب على التقنيات اللاسلكية التي توفر معدلات البيانات السريعة والأداء العالي يتزايد باستمرار. مع ظهور التقنيات اللاسلكية الجديدة مثل 5G والشبكات المركبات والتحول نحو أنظمة متعددة الإدخال ومتعددة المخرجات (MIMO) الواسع، لا بد من أن تستخدم الموارد على النحو الأمثل. التردد المتعامد بالتقسيم (OFDM) هي تقنية واعدة وتستخدم على نطاق واسع في مجال الاتصالات اللاسلكية. مؤخرًا، تم اقتراح مجموعة جديدة من مخططات دعا OFDM مع تعديل المؤشر (OFDM-IM) بناء على أساس تقنية التحوير المكانية (SM). يوفر OFDM-IM أداء أفضل في القنوات اللاسلكية، وأكثر مرونة للتدخل. في هذه الأطروحة، تم تصميم عائلة جديدة من تقنيات OFDM-IM تسمى OFDM مع قفل مؤشر التحويل (OFDM-ISK) وتدرس تأثير التدخل الضيق (NBI) على OFDM-IM. ويظهر من الناحية التحليلية والمحاكاة أن المخططات المصممة حديثًا أفضل أداء من OFDM-IM. وبالإضافة إلى ذلك، يتم تقييم OFDM-IM تحت NBI والمحاكاة توضح أنه على عكس OFDM الكلاسيكية، IM يمكن أن تصمد أمام تأثير NBI إلى درجة أكبر. وأخيرًا، يقترح تقنية التخفيف وتنفيذها لتحسين الأداء في التدخل العالي جدا.

CHAPTER 1

INTRODUCTION

This thesis presents a research done on the topic of Orthogonal frequency Division Multiplexing with Index Modulation (OFDM-IM). OFDM-IM is a recently proposed transmission scheme for wireless communications to improve performance especially in mobile channels [1]. This work is basically concerned with two aspects of OFDM-IM. Firstly, this research proposes a new family of the so called Index Shift Keying (ISK) by coming up with the complete system design and deriving the performance evaluation criteria. The second part covers the impact of Narrowband Interference (NBI) on OFDM-IM and Inter-Carrier Interference (ICI) on ISK. The performance of OFDM-IM with and without mitigation techniques is compared to the performance of OFDM under NBI. The so called ISK techniques are evaluated by simulations when the channel is subjected to ICI. From here on, to refer to both OFDM-IM and family of ISK techniques, this write-up uses the term Index Modulation (IM).

This introductory chapter will give an overview of wireless communications, clas-

sical Orthogonal Frequency Division Multiplexing (OFDM) and how OFDM-IM was derived from Spatial Modulation (SM). It will then provide the motivation behind this work and define the thesis scope and contributions. Some important mathematical terminologies and notations are also introduced. Lastly, the complete thesis structure is provided.

1.1 Introduction to wireless communications

Wireless communications is part of our everyday life in the form of technologies such as Wi-Fi, fourth generation Long-Term Evolution (4G LTE) and Worldwide Interoperability for Microwave Access (WiMAX) to name but a few. Furthermore, newer standards such as fifth generation (5G) networks and Light Fidelity (Li-Fi) are emerging to meet the modern day requirements. The past few years have seen a boom in network usage and there is always a demand for more. Furthermore, people nowadays expect to be connected at all times whether they are at home, work or commuting. This has caused a huge demand for speed and volume in wireless communications. Consequently, researchers and engineers are constantly on the lookout for how to improve these technologies.

Recent communication standards such as WiMAX and 4G LTE make use of MIMO-OFDM techniques in order to achieve the best possible spectral efficiency (SE) and Bit Error Rate (BER) performance [2]. However, these achievements arrive at a cost of energy efficiency (EE). This is not optimum as there is a pressure nowadays to go green. Over the last few years, Spatial Modulation (SM)

schemes have been proposed in order to improve the EE without affecting the SE and performance at the same time [3].

SM-MIMO utilizes all the antennas but only one of them is active at any given instant and the others are switched off. The information is transmitted explicitly via M-ary modulation schemes as well as implicitly via the position of the transmitting antenna. Furthermore, Space Shift Keying (SSK) modulation has been designed such that the information is only transmitted via the position of the antenna [4]. Recently, inspired by the concept of SM, an innovative modulation technique called OFDM with index modulation (OFDM-IM) has been proposed in literature [1]. We will now give a brief historical overview of OFDM and introduce the idea of OFDM-IM. .

1.2 Orthogonal Frequency Division Multiplexing (OFDM)

Frequency Division Multiplexing has been used in radio communication extensively during the last century. The problem was that this method was spectrally inefficient because each channel took over the complete bandwidth in addition to a guard band. Orthogonal FDM (OFDM) was first suggested in the late 1950s in order to eliminate this spectral inefficiency by overlapping the spectrum of all sub-channels [5].

The idea is to ensure that the peak of each sub-channel corresponds to the null of

the sidebands of the adjacent channels. Mathematically, this is possible if all adjacent carriers are orthogonal to each other, hence the name OFDM. Initially, the implementation of such a system was very bulky due to the presence of large filter banks. In 1971, a landmark was reached when Weinstein and Ebert suggested the use of Discrete Fourier Transform (DFT) to implement OFDM [6]. The details of this implementation are provided in section 2.1.

1.2.1 OFDM with Index Modulation (OFDM-IM)

The idea of OFDM-IM is to use a few of the available sub-carriers to transmit actual modulated data symbols. The rest of the information is transmitted via the indices of the active sub-carriers. So in OFDM-IM, the data is modulated as it would be for a typical OFDM transmission. However, only a combination of sub-carriers are used and the information is transmitted via the data as well as the location of these sub-carriers. More details about the work done in the field of OFDM-IM are given in 2.5.2 and a complete overview is provided in chapter 3.

1.3 Thesis Scope and Motivation

The goal of OFDM-IM is similar to SM, where the aim is to maintain BER performance and SE without the added cost of low EE [7]. The distinction is that OFDM-IM achieves that by switching off certain sub-carriers whereas SM applies this mechanism to antennas in Multiple Input Multiple Output (MIMO) systems [1]. OFDM-IM can work with either Single Input Single Output (SISO) or MIMO.

It is important to note that it has a huge potential in massive MIMO systems which will be deployed in wireless standards in the near future. OFDM-IM also performs much better than the classical OFDM in mobile environments. Consequently, it will have an application in the physical layer of the exciting new field of vehicular networks [8]. Therefore there is a demand for studying OFDM-IM itself but also for coming up with even better modulation schemes.

It is expected that IM will be implemented on MIMO systems in combination with SM. Moreover, it is predicted that in the future large-scale MIMO systems will replace small-scale configurations. Therefore these IM schemes need to be tailored to such systems. Furthermore, there is a need to design OFDM based methods that only use sub-carrier index switching to mirror the Space Shift Keying (SSK) techniques used in MIMO. Recently, combined MIMO-OFDM-IM schemes called Space Frequency Modulation (SFM) have been proposed in literature [9]. We propose techniques under the label of Index Shift Keying (ISK) that will be compatible with SSK and large scale MIMO systems.

Although OFDM-IM boosts the performance and EE, the improvement in error performance is not significant enough. Hopefully, by utilizing only sub-carrier positions to modulate the data without any linear modulation will further enhance the performance. In addition, despite the reduction in SE, due to the transmission of lower power overall may provide better EE especially at some SNR ranges or for particular values of SE.

So far, the receivers described in literature assume perfect Channel State Infor-

mation (CSI). It is assumed that the noise follows the Additive White Gaussian Noise (AWGN) model and the channel follows the Rayleigh fading model. The effects of imperfect CSI and Inter-Carrier Interference (ICI) have been studied for OFDM-IM [8]. In addition to ICI, there are other impairments such as partial CSI, Narrowband Interference (NBI) and other types of channel responses such as Rician and Nakagami fading. NBI is of special importance because of the overloading of radio frequency bands (especially between 1GHz - 30GHz). This can result in unintentional jamming of a few sub-carriers in the range of operation. There can also be intentional jamming in sensitive environments such as military applications [10]. Thus, it is vital to study the effects of such impairments in OFDM-IM or any new systems based on IM.

1.4 Thesis Contributions

In this research, novel variations of the OFDM-IM are designed and evaluated, the effects of NBI on the performance of OFDM-IM are studied and a mitigation method is examined. The thesis is divided mainly into two parts: design and evaluation of IM related modulation techniques and the study of the impact of NBI on the original OFDM-IM and ICI on ISK. The contributions are listed below in detail:

1. Design of a new family of modulation methods called Index Shift Keying including the:
 - (a) transmitter and receiver design for the new techniques

- (b) analytical performance evaluation
 - (c) comparisons with analytical results and IM
2. Characterize and mitigate the impact of NBI on IM techniques by:
- (a) studying the performance degradation with respect to the number of affected sub-carriers
 - (b) discussing the role of interference power in the performance degradation
 - (c) proposing a mitigation technique based on compressed sensing and comparing the results with unmitigated cases
3. Examine the immunity of IM techniques to ICI as compared to OFDM by:
- (a) characterizing the ICI with respect to IM techniques
 - (b) studying the impact of ICI with simulations on ISK.

1.5 Thesis Organization

The thesis is arranged into six chapters according to the following structure:

Chapter 1 introduces the subject material, describes and the problems motivations behind tackling them and highlights the main contributions.

Chapter 2 provides background information on classical OFDM and how the concept of Spatial Modulation in MIMO systems led to OFDM-IM. This chapter also provides a comprehensive literature review on previous research carried out in this area.

Chapter 3 reviews the original so called OFDM-IM technique by describing the transmission model, receiver architecture and the performance evaluation by simulations compared to the analytical results and classical OFDM methods.

Chapter 4 introduces the newly proposed so-called family of ISK techniques, their transmitter/receiver architectures, analytical performance evaluation and simulation results.

Chapter 5 evaluates the impact of ICI and NBI on IM techniques. A study is conducted on the significance of the number and power of NBI signals. The performance degradation of IM techniques with respect to these parameters is studied in great depth. Moreover, a mitigation strategy is employed and its effectiveness is discussed. A review of the effects and mitigation methods of ICI in OFDM-IM is performed along with the comparisons with the ISK techniques and classical OFDM with the help of simulations.

Chapter 6 concludes the research done and provides insight into the possible future research directions in OFDM-IM.

1.5.1 Important Notations

Matrices are denoted by bold-faced capital letters whereas small bold-faced letters denote column vectors. Vectors and Matrices in time-domain (TD) are subscripted with T and F is used a subscript for the frequency domain (FD). For example, \mathbf{X}_F and \mathbf{x}_T represent a matrix \mathbf{X} in FD and a column vector \mathbf{x} in TD, respectively. $x(j)$ represents the j^{th} element of the vector. The acronyms pdf and RV are

used for the probability density function and random variable, respectively. The Fourier Transform and inverse Fourier Transform operations are denoted by \mathcal{F} and \mathcal{F}^{-1} , respectively. A circularly symmetric complex normal RV n with mean μ and variance σ_n^2 is given by $n \sim \mathcal{CN}(\mu, \sigma_n^2)$.

The set of complex numbers is represented by the scripted letter \mathbb{C} where $\mathbf{X} \in \mathbb{C}^{N \times M}$ is an $N \times M$ complex matrix. The expression $\mathbf{x} = \text{diag}(\mathbf{X})$ refers to a vector that is formed by the diagonal elements of the matrix \mathbf{X} . In contrast, $\mathbf{X} = \text{diag}(\mathbf{x})$ is a diagonal matrix whose components are the elements of the vector \mathbf{x} . The $N \times N$ identity and all zero-matrices are given by \mathbf{I}_N and $\mathbf{0}_N$, respectively. The determinant of the matrix \mathbf{X} is given by $\det(\mathbf{X})$. The expressions \mathbf{X}^T , \mathbf{X}^H and \mathbf{X}^{-1} refer to the transpose, Hermitian transpose and matrix inverse of \mathbf{X} , respectively.

CHAPTER 2

BACKGROUND AND LITERATURE REVIEW

In this chapter, we present a theoretical background and a literature review of OFDM-IM and other relevant technologies. We begin by giving a brief historical overview of OFDM as well as the necessary theoretical background. The problem of interference is then discussed especially how it affects to modern day systems. A brief overview of MIMO systems is given leading to the discussion of SM and SSK. A few of the pioneering papers are mentioned. Once that is covered, a comprehensive literature survey of OFDM-IM is presented.

2.1 OFDM

In the modern day implementation of OFDM, L modulated symbols are divided into L/N parallel groups of N symbols that represent the frequency domain data. N -point Inverse Fast Fourier Transform (N-IFFT) is applied where N also denotes

the number of sub-carriers available. Additional enhancements such as the use of the cyclic prefix and interleaving are made before the IFFT process. For wireless communications, an added advantage is that OFDM is immune to frequency selective fading where different frequency components undergo uncorrelated fading. [11].

OFDM can effectively negate this type of fading by converting a large frequency band into to N Rayleigh flat fading channels, where the frequency response can be assumed constant for that particular band. In order to achieve this and to prevent interference between successive transmissions, a guard interval in time domain (TD) or equivalently a few guard bands are added in the frequency domain (FD). The number of channel 'taps' should not exceed the length of the guard bands by one [11, 12].

Many approaches have been used in order to design these guard bands. One such method involves adding a cyclic prefix (CP), where the last L_{cp} components of the transmission vector are added to the beginning of the frame. Another technique is zero padding which as the name suggests, involves the insertion of zeros instead of the tail of the transmitted data. A cyclic suffix may also be added. From circular convolution, we know that the signal can be recovered by simply discarding the extra frames in case of CP, and by adding the tail to the header in case of zero-padding [11, 13]

2.2 Narrow-band Interference

Narrow Band Interference (NBI) refers to interference with a spectrum that is far less than the spectrum of the transmitted signal. In OFDM systems, NBI occurs mainly due to the existence of the unlicensed Industrial, Scientific, and Medical (ISM) bands. For example, OFDM WLANs (WiFi mainly) suffer from interference that occurs due to devices operating in the same band such as microwave ovens and Bluetooth. The performance degradation due to NBI usually occurs at the receiver just before demodulation. It can ruin the performance of many sub-carriers and cause a serious degradation of Signal to Noise Ratio (SNR) at the sub-carrier closest to the interferer frequency [10]. Detailed mathematical models are presented in chapter 5; for now we review some of the work done on NBI cancellation in literature.

In order to perform demodulation correctly, it is important to mitigate the effects of NBI. Various techniques have been proposed in literature to combat NBI. Some of these methods include frequency excision, interference cancellation, adaptive narrowband filtering, LMS algorithms and wavelet denoising [10]. However, these techniques mostly tackle non-fading AWGN channels. A structured approach based on ML decoding is presented by Sohail et al. for zero padded OFDM [14]. The work of [15] tackles NBI using a compressive sensing (CS) based approach. The sparse nature of the NBI is exploited by carrying out sparse recovery using the algorithm known as support agnostic Bayesian matching pursuit (SABMP).

Recently, further work has been done by Gomaa et al. the area of using CS

techniques based on convex optimization in order to solve the problem of NBI. In 2010, two approaches, one based on guard interval redundancy in ZP-OFDM and another based on multiple receivers is used to cancel NBI in non-fading channels [16]. Gomaa and Aldhafer apply the CS based technique to the case of a mobile jammer and CP-OFDM [17]. The work is then extended for MIMO-OFDM and a channel estimation technique is proposed [18]. Finally, the cases of fast and frequency selective fading in MIMO-OFDM channels are tackled in [19].

2.3 MIMO

Multiple Input Multiple Output (MIMO) refers to a system that utilizes multiple antennas for transmission and reception. MIMO systems can help achieve higher bit rates through spatial multiplexing or higher error performance through diversity techniques. In multiplexing, multiple symbols can be transmitted at the same time over the same frequency by exploiting the spatial difference between the antennas. A famous family of MIMO multiplexing techniques is the Bell-Labs Layered Space-Time Architecture (BLAST). Two of the commonly used variation in literature are the Vertical-BLAST (V-BLAST) and the Diagonal-BLAST (D-BLAST).

Diversity involves redundant transmissions of the signal in the spatial domain without affecting the spectral efficiency or the bit-rate compared to single antenna systems. Diversity can be due to obstacles that occur between transmitters and receivers (macroscopic) or due to multipath fading via scatterers (microscopic) [20].

Diversity techniques can be applied to the receiving side such as maximum ratio combining (MRC), Equal Gain Combining (EGC) and Selection Diversity (SD). Transmit diversity results from sending the same signal over multiple channels redundantly. A significant development is that it can be combined with coding schemes in order to achieve coding gains without extra overhead. Space Time Block Codes (STBCs) such as the Alamouti STBC or Space Time Trellis Codes (STTCs) can be applied prior to transmission in order to improve the performance [20].

2.4 Spatial Modulation

As it can be observed from previous sections, MIMO technology utilizes multiple antenna elements (AE's) at the transmitter and/or receiver as well as the resulting multiple RF chains (RFC's) because all AE's are active at any given time. Although this method significantly improves Spectral efficiency (SE) and BER performance, it comes at a cost of Energy efficiency (EE) and higher complexity at the receiver especially in the case of large-scale MIMO. Spatial Modulation (SM) techniques were designed to take advantage of the MAE but reduce the system to one RFC only at any given instant. Therefore the diversity and multiplexing advantages of conventional MIMO are retained without the added cost of EE [21].

2.4.1 SM Review

The concept of SM was first introduced by Mesleh et al in 2006 as a way to remove Inter Channel Interference from the receiver totally [3]. The need for synchronization between transmitters was eliminated while maintaining the SE [3]. The Symbol Error Rate (SER) of SM is analyzed using statistical and M-ary orthogonal detection approaches in uncorrelated Rayleigh fading channels in [22]. The impact of channel estimation errors is discussed in [23] and [24]. The research in [23] covers SM whereas the work of [24] discusses other techniques such as SSK (covered in the next sub-section); both analyses assume the error model to be complex Gaussian.

Using SM, capacity can also be enhanced due to the exploitation of the spatial domain. However, the drawback is that the data rate is only enhanced proportional to the base two logarithm of transmitting antennas compared to other SMX techniques where it enhances linearly with the number of transmitting antennas. Quadrature SM (QSM) is suggested by Mesleh and Ikki [25] in order to overcome this deficiency where another component is added in the signal constellation domain to include in-phase and quadrature-phase components [25, 26]. Similar to SM, one group of bits is used to select the antenna index and in contrast to SM, two groups of bits are mapped on to the signal constellation using two quadrature out-of-phase carriers.

2.4.2 SSK Review

Space Shift Keying (SSK) was first introduced as Generalized SSK (GSSK) by Jeganathan et al [27]. In contrast to SM, the idea was to transmit information using only the antenna indices without any form of M-ary Amplitude/Phase modulation. It was designed such that n_t out of N_t transmit antennas would be active. A sequence of ones is sent through those AEs (normalized to unit energy) and the combination would be used to predict the transmitted symbol (bits). GSSK led to reduction in the receiver complexity and led to an improved BER performance by increasing the distance between the constellation points through the channel's fading characteristics. Although a promising innovation, GSSK failed to take advantage of the transmitted energy fully. A modified Generalized Phase SSK (GPSSK) was proposed where two symbols would utilize the same AEs but transmit different phases [28]. In this way, the benefits of SSK are retained with an increased efficiency.

The work of [4] proposes SSK which is a specific case of GSSK where the number of transmitting antennas are to the base two (e.g. 2, 4, 8, etc.). In this case, a binary one is simply transmitted on the antenna with the index corresponding to incoming symbol. The detection complexity is further lowered and this scheme can be utilized in technologies that use pulse transmissions such as UWB. The error performance is analyzed for coded and uncoded cases as well as for ideal channels and non-ideal channels with CSI errors and spatial correlation. Further analysis is performed in non-ideal channels by Renzo and Haas where they exam-

ine SSK in channels that suffer from Rician fading and where only partial CSI (P-CSI) is available [29, 30]

2.4.3 SM-OFDM

It is clear that SM and OFDM are both promising techniques for wireless communications and both schemes can be combined to retain the benefits of each [31]. SM-OFDM is done by applying SM to OFDM explicitly by first performing SM on the received bits and then applying OFDM at each transmitter. The application OFDM is done in parallel such that all sub-carriers are used at any given antenna. MRC is applied at the receiver side in order to extract the antenna number and then to demodulate the received symbols [32]. It is shown that SM-OFDM outperforms classic STBC based Alamouti and V-Blast MIMO-OFDM schemes. The impact of channel imperfections including Rician fading, spatial correlation and mutual coupling is discussed in [33].

2.5 OFDM-IM

Using the concept of spatial modulation, researchers combined it with the OFDM method to create a family of modulation techniques called Index Modulation. Figure 2.1 summarizes the research done related to the area OFDM-IM. In the following sections, we will provide a comprehensive review about the work done on OFDM-IM so far and explore every aspect.

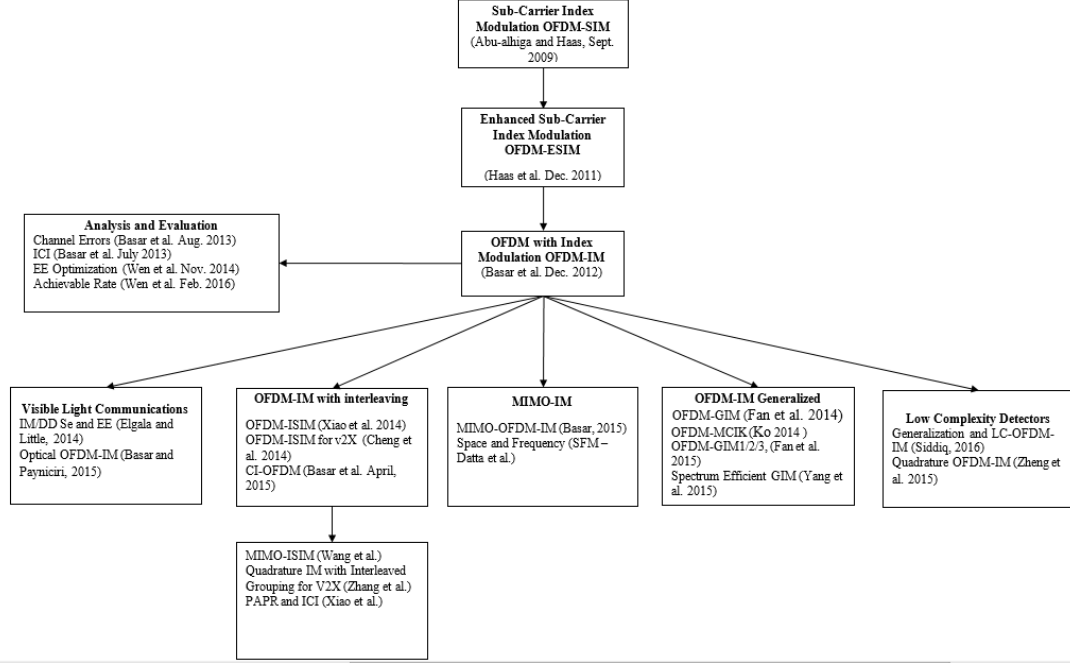


Figure 2.1: Illustration of the work done on OFDM-IM in literature

2.5.1 Sub-Carrier Index Modulation

Abu-alhiga and Haas [34] proposed the concept of Subcarrier-Index modulation OFDM (SIM-OFDM). Usually, OFDM is performed on M -ary modulated symbols directly. Therefore N symbols or $N \times \log_2 M$ bits are mapped onto N subcarriers using N -point FFT.

In the proposed scheme, the incoming data consisting of $N(\log_2 \frac{M}{2} + 1)$ is split into two streams. One stream of $N \log_2 M/2$ bits is used to generate the M -ary symbols whereas the other stream of size N bits is used to choose the sub-carrier as follows. Firstly, it is decided which of the bits are in the majority, 0's or 1's. Once that is discovered, the index of the subcarrier is chosen using On-Off Keying (OOK) depending on the majority bit. This means that if there are more zeros, all sub-carriers corresponding to the position of the zeros will be activated and vice

versa. Unless zeros and ones are equal in number, there may be excess activated sub-carriers that can be used to signal the majority bit.

The status of each sub-carrier can be predicted using a coherent OOK detector but the status of the activating bit (0 or 1) is still unknown. The received symbols are demodulated to the corresponding M-ary constellation. Using forward error control mechanisms and combining the demodulated data with both hypotheses (0 and 1), the status of the activating bit stream (0 or 1) can be postulated. The paper then goes on to describe two separate power allocation schemes that provide a trade-off between spectral and power efficiency. The BER of the SIM-OFDM is also analyzed in Rayleigh flat fading channels. By simulations, it is proved that the SIM-OFDM gives better results than the conventional OFDM [34].

Although promising, SIM suffers from error propagation that can lead to burst errors. In order to avoid that, a new enhanced SIM-OFDM (ESIM-OFDM) was developed by Haas et al [35]. In ESIM-OFDM, $N/2$ bits are used to indicate the active sub-carriers by encoding one bit into a pair sub-carriers as follows. If a binary zero is encountered, the first of the two subcarriers is switched on and the second one is switched off and vice versa for a binary one. This ensures that one of every two consecutive sub-carriers is inactive. Consequently, an error in the decoding of one active index during demodulation will not affect how the next index is decoded. Hence, the problem of error propagation is avoided. In addition to suppressing burst errors, ESIM-OFDM provides the advantage of reducing the peak to average power ratio (PAPR) [35].

2.5.2 OFDM with Index Modulation

From section 2.5.1, it is apparent that the initial index modulation methods did not allow for freedom of choosing the number of active sub-carriers. Moreover, the SIM-OFDM algorithm presented in [34] results in an unequal number of active sub-carriers per OFDM block. Therefore to indicate the mapping sequence, perfect feedforward signaling is assumed which is too optimistic for a realistic channel. This problem was fixed in [35] but the solution requires very high order modulations in order to achieve a comparable spectral efficiency to classical OFDM. There was also no flexibility in selecting the number of sub-carriers either; for example according to best performance.

Building on the previous techniques, Basar et al [1] designed a form of index modulation (OFDM-IM) that gives more freedom in choosing the active sub-carrier indices [1, 8]. N carriers are divided into groups of n which consists of k active sub-carriers. The values n and k can be chosen to provide the best Quality of Service (QoS) in terms of performance, spectral efficiency or complexity. Another benefit is that the exploitation of the OFDM-IM spatial domain provides higher diversity thus enhancing the BER performance by taking advantage of the frequency selectivity[1].

The work in [1] introduced the concept of OFDM-IM and introduces two distinct implementation techniques. For any sub-block k carriers out of n are active with $C(n, k)$ combinations possible. For any value of n and k , $\lfloor \log_2 C(n, k) \rfloor$ can be assigned using a look-up table or combinatorial mathematics (which is useful for

large k and n values). Two different receivers were designed, ML detector and Log-Likelihood Ratio (LLR) detector for each transmission technique, respectively. In addition, an expression for the upper bound of the Unconditional Pairwise Error Probability (UPEP) was derived.

For SNR higher than 15 dB for $n = 4$ and $k = 2$, OFDM-IM performed better than classical OFDM using the ML receiver and the simulation BER approached the theoretically derived curve. For higher values of n and k , the LLR receiver was employed and performed similar to lower rate OFDM at high SNR values. Lastly, LLR decoder was employed for the case without M-ary modulation (data is encoded only in the sub-carrier similar to SSK) and it provided the highest diversity order.

The work of [8] applied the same modulation techniques in a highly mobile channel. Four separate types of detectors were proposed: Minimum Mean Square Error (MMSE) in conjunction with LLR/ML, sub-matrix, Inter Channel Interference (ICI) self-cancelling block and Signal Power (SP) detectors. The SP detector provided the best performance in general whereas OFDM-IM offered better BER performance even for much higher data rates.

Finally, [1] summarized all of the cases and performed detailed experiments on various detectors in addition to two new contributions. Firstly, a new LLR+ML detector was presented that achieved lower complexity at the cost of slightly sub-optimal detection. Secondly, an expression for the upper bound of the Conditional Pairwise Error Probability CPEP was derived under channel estimation errors and

a new mismatched ML decoder was suggested for that case. The research in [1] is the basis for this thesis and the detailed implementation of the OFDM-IM algorithm is presented in chapter 3 along with the analyses and results of some of the cases relevant to this thesis. Prior to that, the following sections present a review of further work done on OFDM-IM.

2.6 MIMO-OFDM-IM

Basar proposed the so called MIMO-OFDM-IM as a new scheme for 5G communications as a replacement to existing MIMO-OFDM [36]. A group of $N_T \times B$ bits are transmitted using N_T transmit antennas and N_R receive antennas. The B bits are modulated using the OFDM-IM technique and sent using N_T transmitters. Two detection schemes are proposed: the ML detector and a lower complexity combination of a modified MMSE+LLR detectors. It is shown that the OFDM-IM perform better than classical OFDM with MIMO for all configurations.

Datta et al. propose a combined space-frequency modulation scheme [9]. They first modify GSM to generalized spatial index modulation (GSIM) and show that it can achieve higher rates than MIMO-OFDM. Then they design a combined spatial-frequency index modulation (GSFIM) where the information is transmit via the active antennas, sub-carriers and modulated bits. It is shown that such a scheme provides very high achievable rates. MIMO configurations are also used in conjunction with interleaved OFDM-IM [37]. A more detailed review is given in section 2.8.

2.7 Generalized OFDM-IM

A generalized version OFDM-IM called Generalized Index Modulation (OFDM-GIM) removed the constraint of a fixed number of active sub-carriers per sub-block. Increasing the number of sub-carriers increased the spectral efficiency at a slight cost of BER performance and a more complex LLR detector. The complexity of the LLR decoder increases because the number of active sub-carriers have to be determined for each sub-block; which means synchronization is needed [38]. An enhanced version of OFDM-GIM is proposed by Yang et al. [39] which links the modulation used to the number of active sub-carriers, resulting in improved performance.

Fan, Yu and Guan designed three new schemes to further generalize the structure of OFDM-IM. They named these schemes OFDM-GIM1, OFDM-GIM2 and OFDM-GIM3 [40]. OFDM-GIM1 relaxes the constraint on the number of active sub-carriers in each block. On the other hand, OFDM-GIM2 relies on a constant number of active sub-carriers but transmits using in-phase and quadrature components. A trade-off between the Spectral Efficiency (SE) and BER performance is achieved as more bits can be transmitted per sub-block compared to OFDM-IM but at a cost of performance.

In order to improve the BER performance, interleaving is used. GIM1 and GIM2 are then combined along with interleaving to form the so called OFDM-GIM3. It is shown that GIM3 provides better performance in terms of the SE and BER. A low complexity OFDM-IM (LC-OFDM-IM) is proposed by Siddiq to reduce detec-

tor complexity in a similar approach to GIM1. The analysis is done for non-fading channels suffering from AWGN only such as optical wireless communications. It is shown that LC-OFDM-IM can replace the OFDM-IM with ML detector with a degradation in BER performance [41].

2.8 Interleaved OFDM-IM

It was observed that OFDM-IM offers better BER performance only for low SNR values. To improve performance for high power channels, a family OFDM-IM techniques in conjunction with interleaving have been discussed in the literature. The authors of [42] have introduced a simple block interleaver of depth equal to the number of sub-blocks. Every symbol is grouped with a symbol corresponding to its position in all other sub-blocks after OFDM-IM to form then so called OFDM with interleaved SIM (OFDM-ISIM). This method resulted in an increased Average Euclidean Distance (AED) and minimum ED (MED). Consequently, the BER performance was improved.

A similar approach was applied in [43] but specifically for the case of vehicle to X (V2X) networks that suffer from very high mobility. An added advantage of interleaving is that it reduces the correlation between the channels of sub-carriers as a result of the carriers spacing being larger than the coherence bandwidth. The results show that the BER curve was lower and the maximum achievable rate and throughput higher for OFDM-ISIM than OFDM-IM in V2X channels. The work of [44] introduced OFDM-IM using Coordinate Interleaving (CI-OFDM) which is

in contrast to the work of [42] and [43] because the interleaver is applied to the M-ary symbol. A square M-QAM modulation is assumed and before OFDM-IM is applied, the symbols are coded in a manner similar to the Alamouti 2×2 STBC.

Zhang et al. combined the works of [40, 43] to develop the framework for Quadrature Index Modulated Index Modulated OFDM (IQIM-OFDM) with interleaved grouping for V2X channels. Practical experiments were carried out by simulations for vehicles traveling in various environments. It was shown that IQIM-OFDM gives better results in terms of both, the SE and BER performance [45]. Zheng et al. then proposed a lower complexity detector for this method which they term OFDM-I/Q-IM [46].

The work of Wang and his colleagues came up with an implementation of the ISIM technique designed by [42] on MIMO systems. ML detection and modified MMSE detection was proposed for the receiver. It is shown that MIMO-ISIM provides considerably better performance than MIMO-OFDM technology.

2.9 OFDM-IM Evaluation

Some research was carried out on evaluating the performance of OFDM-IM and its variants from various aspects. OFDM-IM performance under imperfect CSI (by analysis) and ICI (by simulations) has been evaluated in [1]. As mentioned previously though, the work of [1] only resulted in PEP expressions for the ML detector case in perfect and imperfect channels. Youngwook Ko derived the closed-form

expression for the BER upper bound for the general case of the so called Multi-Carrier Index Keying (MCIK) for OFDM consisting of M active sub-carriers for the reduced complexity ML detector. The resulting expression was a tight union bound of errors that occur due to the correct and wrong detection of indices, respectively [47].

The achievable rate of OFDM-IM was investigated in [48] by Wen and his colleagues. They first propose an interleaved method for sub-carrier grouping and show how it enhances the performance. They then investigate the impact of modulation types on the ergodic capacity of OFDM-IM. It is proven that OFDM-IM achieves higher rates with Phase Shift Keying (PSK) compared to classical OFDM. In contrast, Quadrature Amplitude Modulation (QAM) does not offer a large improvement. Xiao et al. investigated the peak-to-average power ratio (PAPR) of ISIM and the performance in the presence of ICI. It is shown that ISIM reduces the PAPR and is more robust to ICI than classical OFDM.

Wen, Cheng and Yang investigated the energy efficiency (EE) performance of OFDM-IM and came up with an analytical expression [7]. It is proved that the EE is inversely proportional to the channel correlation and also depends on the link between the number of active sub-carriers and modulation type. Based on the results, a couple of strategies were proposed to optimize OFDM-IM EE. Using interleaved sub-carrier grouping (similar to the approach of [42, 43]) as opposed to the localized grouping (such as in [1]) and carefully choosing the modulation type can optimize the EE performance of IM.

2.10 OFDM-IM for Visible Light Communication (VLC)

As described previously, OFDM-IM has potential applications for optical wireless communications (OWC), specifically VLC and Light-Fidelity (Li-Fi). Basar and Panayirci propose Optical-OFDM-IM (O-OFDM-IM) as a trans-receive scheme for VLC [49]. Simulations are carried out by modeling a typical VLC channel for a room. Results show that O-OFDM-IM performs better than existing OFDM techniques for OWC. A novel Spectral and Energy Efficient OFDM (SEE-OFDM) approach is designed by Elgala and Little that offers reduced PAPR while improving the SE and EE [50].

2.11 Summary

This chapter provides a background on OFDM and reviews the work done so far in the area of OFDM-IM. We begin by describing an OFDM system and introducing the NBI problem as well as mentioning some of the NBI cancellation methods in literature [14]-[19]. A brief background on MIMO systems is provided and an overview of SM and SSK is given. Section 2.5 then explains in detail how OFDM-IM [1] was introduced to improve on the existing SIM-OFDM [34] and ESIM-OFDM [35]. The remaining sections review the work done on MIMO-OFDM-IM [36, 37], Generalized OFDM-IM [38]-[40], Interleaved OFDM-IM [42]-[45] and analytical evaluation [47, 48] of various aspects of OFDM-IM.

CHAPTER 3

REVIEW OF OFDM-IM

In section 2.5, a comprehensive survey and theoretical introduction to various sub-carrier index modulation techniques were presented. In this chapter, we focus on the system model for OFDM-IM and introduce the system block diagram. In addition, the maximum likelihood (ML) receiver for the case of perfect CSI (no channel estimation errors) is presented.

3.1 OFDM-IM System Model

Let us denote the total number of sub-carriers by N and the number of sub-blocks by G . In that case n , the number of sub-carriers per sub-block is given by

$$n = \frac{N}{G}. \quad (3.1)$$

For any given sub-block, only k out of n sub-carriers are utilized. The first b_i bits in each sub-block are used to determine the position of the active sub-carriers

whereas the remaining b_s bits are mapped to $\log_2 M$ symbols of a M-ary Amplitude/Phase modulation. Assuming that the total number of bits transmitted by one OFDM block are given by B , the number of bits transmitted by one sub-block b_t can be given by

$$b_t = \frac{B}{G} = b_i + b_s. \quad (3.2)$$

and therefore b_i and b_s can be determined using 3.3 and 3.4, respectively, where b_i bits are for index selection and b_s are used for modulation.

$$b_i = \lfloor \log_2(C_{nk}) \rfloor. \quad (3.3)$$

$$b_s = k \times \log_2 M. \quad (3.4)$$

The total number of possible combinations of active sub-carrier arrangements C_{nk} within a sub-block are

$$C_{nk} = \binom{n!}{k!(n-k)!}. \quad (3.5)$$

However, since the number of sub-carriers is selected using a combination of the first b_i bits, the actual possible combinations C has to be of base two as in 3.6 and there are C_{un} unused combinations as given in 3.7.

$$C = 2^{b_{si}} = 2^{\lfloor \log_2(C_{nk}) \rfloor}. \quad (3.6)$$

$$C_{un} = C_{nk} - C. \quad (3.7)$$

After all sub-blocks are passed through the index selector and M-ary modulator, the indices of the active sub-carriers and the modulated signal are given by the matrix \mathbf{I} and vector \mathbf{s} , respectively,

$$\mathbf{I} = [\iota_{g,1} \ \iota_{g,2} \ \dots \ \iota_{g,k}] \quad (3.8)$$

$$\mathbf{s} = [s_{g,1} \ s_{g,2} \ \dots \ s_{g,k}] \quad (3.9)$$

where $\mathbf{i}_{g,\gamma} \in \{1, \dots, n\}$ and $\mathbf{s}_g(\gamma) \in \mathbb{S}$ for $g = 1, \dots, G$ and $\gamma = 1, \dots, k$. The total number of active carriers in the whole OFDM block is $K = kG$. The total number of bits used to select the active sub-carriers B_{ind} is given by $b_i G$ and the total number of modulated bits are B_{mod} given by $b_s G$. The total number of bits B is equal to $B_{ind} + B_{mod}$. The assumption is made that the average power of the signal constellation is normalized to unity as illustrated in 3.10.

$$E[\mathbf{s}_g^H \mathbf{s}_g] = 1 \quad (3.10)$$

The frequency domain OFDM block $\mathbf{x}_F = [x_F(1) \ x_F(2) \ \dots \ x_F(N)]^T$ where $x_F(j) \in \{0, S\}, j = 1, \dots, N$. Figure 3.1 describes the complete system design of OFDM-IM.

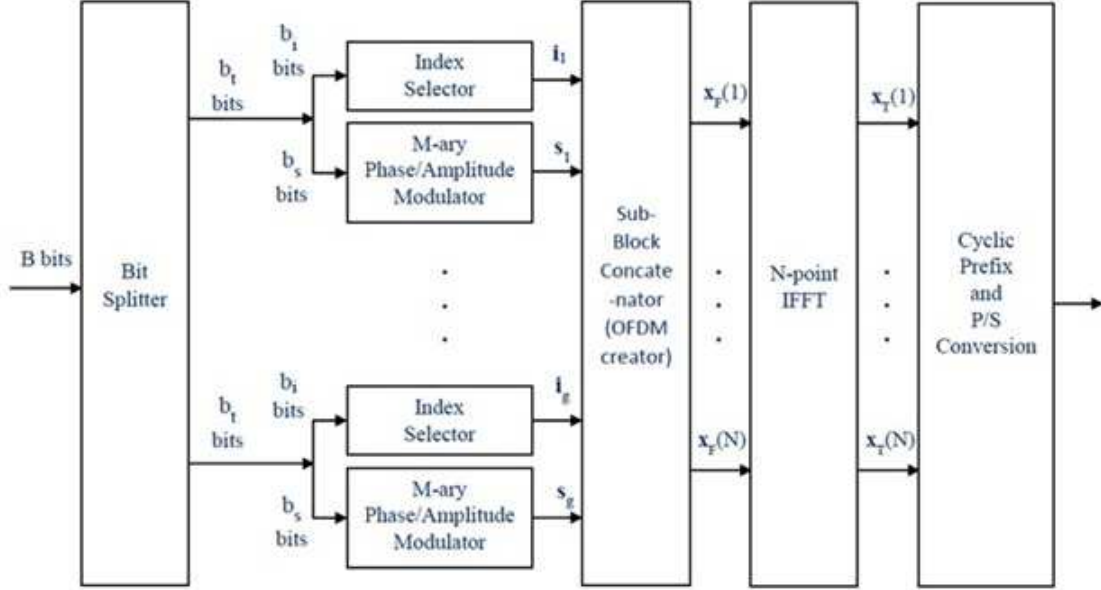


Figure 3.1: Block Diagram of the OFDM-IM block generator

3.2 Look-Up Table Implementation

As it has been explained in section 2.5.2, there are two implementation methods for the index selector: look-up table and combinatorial mathematics. Since the ML detector works with the look-up table and is the benchmark, only the look-up table method is discussed here. As mentioned in 3.1, B incoming bits are split into G groups of b_t bits and N carriers can be sorted into G groups of n sub-carriers. It is possible to set G as 1, so then there is only one block. However, the receiver complexity will be very high in that case. In any event, the first b_t bits of any sub-block are used to select the carrier indices and the rest of the b_s bits are modulated using linear modulation techniques [1].

In Table 3.1, the case of $n = 4$, $k = 2$ and $C = 4$ (from 3.6) is illustrated. The complete set of possible combinations for such a system with the stated parameters

Table 3.1: An example of index selection for $n = 4$ and $k = 2$

Bits	Indices	Sub-block Structure
00	$\{1, 2\}$	$[\mathbb{S}_1 \ \mathbb{S}_2 \ 0 \ 0]^T$
01	$\{2, 3\}$	$[0 \ \mathbb{S}_1 \ \mathbb{S}_2 \ 0]^T$
10	$\{3, 4\}$	$[0 \ 0 \ \mathbb{S}_1 \ \mathbb{S}_2]^T$
11	$\{1, 4\}$	$[\mathbb{S}_1 \ 0 \ 0 \ \mathbb{S}_2]^T$

Table 3.2: OFDM-IM parameters for $N = 16$ carriers with $n = 4$, $k = 2$ and $M = 4$

Parameter	Value	Equation Used
N	16	—
n	4	—
k	2	—
G	4	(3.1)
b_i	2	(3.3)
b_s	4	(3.4)
b_t	6	(3.2)
B	24	(3.2)
Incoming bit input	100001 110110 011100 001101	

are $\{\mathbf{I}_g | \mathbf{I}_g \in \{1, 2\}, \{1, 3\}, \{1, 4\}, \{2, 3\}, \{2, 4\}, \{3, 4\}\}$ for $g = 1, \dots, G$. Table 3.1 only displays the selection of $C = 4$ out of a possible $C_{nk} = 6$ combinations that are used to create \mathbf{I}_g in this example.

Let us consider an example of a system that uses 16 carriers or $N = 16$ divided into $G = 4$ groups such that $n = 4$ and k is chosen to be 2 for the 4-QAM modulation scheme. Using (3.3) and (3.4), $b_i = 2$ and $b_s = 4$. All of the relevant parameters and an example of an incoming stream of bits are listed in Table 3.2. Table 3.3 is an example of a complete OFDM-IM block created using the look-up table presented in Table 3.1.

Table 3.3: Examples of sub-blocks generated for the system and input bits described by Table 3.1 and look-up table described by Table 3.2

Parameter	b_i bits	b_s bits	sg	ig	$\mathbf{x}_F(g[n-1] + gn)$ for $g = 1, \dots, G$
Sub-Block 1	10	0001	$\{-1 + j, -1 - j\}$	$\{3,4\}$	$\{0, 0, -1 + j, -1 - j\}$
Sub-Block 2	11	0110	$\{-1 - j, +1 + j\}$	$\{1,4\}$	$\{-1 - j, 0, 0, +1 + j\}$
Sub-Block 3	01	1100	$\{+1 - j, -1 + j\}$	$\{2,3\}$	$\{0, +1 - j, -1 + j, 0\}$
Sub-Block 4	00	1101	$\{+1 - j, -1 - j\}$	$\{1,2\}$	$\{+1 - j, -1 - j, 0, 0\}$
One Frame	$\{0, 0, -1 + j, -1 - j, -1 - j, 0, 0, +1 + j, 0, +1 - j, -1 + j, 0, +1 - j, -1 - j, 0, 0\}$				

3.3 ML Receiver implementation

The ML receiver has been proposed to detect OFDM-IM signals with the look-up table technique. The assumption is that perfect CSI is available, the length of the applied cyclic prefix (L_{cp}) is greater than the number of multipath components (or channel taps - L_{ch}) and the channel only goes through slow frequency selective fading, i.e. Rayleigh fading model is assumed.

As illustrated in Fig. 3.1, once the $N \times 1$ OFDM block is created, Inverse Fast Fourier Transform (IFFT) is applied to form the time-domain block

$$\mathbf{x}_T = \frac{N}{\sqrt{K}} \mathcal{F}^{-1}\{\mathbf{x}_F\} = \mathbf{W}_N^H \mathbf{x}_F \quad , \quad (3.11)$$

where the Discrete Fourier Transform (DFT) matrix \mathbf{W}_N is defined such that

$$\mathbf{W}_N^H \mathbf{W}_N = N \mathbf{I}_N \quad (3.12)$$

and a factor of $\frac{N}{\sqrt{K}}$ is used to normalize the OFDM frame energy in time-domain to $E[x_T^H x_T] = N$. At the receiver, a normalization factor of $\frac{\sqrt{K}}{N}$ is employed to recover the OFDM block in the frequency domain.

A cyclic prefix of length L_{cp} such that $L_{cp} > L_{ch} + 1$ is added so that the time-domain vector becomes $[x_T(N - L_{cp} + 1), \dots, x_T(N)]$. After parallel to serial conversion, The signal is passed through the channel defined by the impulse response

$$\mathbf{h}_T = [h_T(1) \ h_T(2) \ \dots \ h_T(L_{ch})]^T \quad (3.13)$$

where $\mathbf{h}_T(l_{ch})$ is a circularly symmetric complex Gaussian Random Variable (RV) with the distribution $\mathcal{CN}(0, \frac{1}{L_{ch}})$ for $l_{ch} = 1, \dots, L_{ch}$.

Based on the assumptions stated above, the received signal vector in the frequency domain can be described as

$$y_F(\beta) = x_F(\beta)h_F(\beta) + w_F(\beta), \quad \beta = 1, \dots, N, \quad (3.14)$$

where $y_F(\beta)$ is an element of the received vector in the frequency domain \mathbf{y}_F . The channel fading coefficients in the frequency domain $h_F(\beta)$ follow the distribution $\mathcal{CN}(0, 1)$ whereas the noise samples $w_F(\beta)$ follow the distribution $\mathcal{CN}(0, N_{0,F})$. The noise variance in the frequency domain is related to the noise variance in time-domain by

$$N_{0,F} = \frac{K}{N} N_{0,T}. \quad (3.15)$$

3.3.1 ML Receiver Architecture

The ML decoder works by performing an exhaustive search of all possible signal constellations over all of the possible combinations of receive indices. Assuming availability of perfect CSI, it works by minimizing the metric

$$\left(\tilde{\mathbf{I}}_g, \tilde{\mathbf{s}}_g\right) = \arg \min_{\hat{\mathbf{I}}_g, \hat{\mathbf{s}}_g} \sum_{j=1}^k |y_F^g(\mathbf{i}_{g,j}) - h_F^g(\mathbf{i}_{g,j})s_g(j)|^2, \quad (3.16)$$

where for the g^{th} sub-block, $y_F^g(\zeta) = y_F(n(g-1)+\zeta)$ and $h_F^g(\zeta) = h_F(n(g-1)+\zeta)$ for $\zeta = 1, \dots, k$ and $g = 1, \dots, G$. The receiver is of complexity $\sim O(cM^k)$ in terms of the complex computations. The SNR of the received signal ρ , the average energy per bit E_b and the SE in bits/sec/Hz are given by (3.17) - (3.19)[1].

$$\rho = \frac{E_b}{N_{0,T}} \quad (3.17)$$

$$E_b = \frac{N + L_{cp}}{B} \quad (3.18)$$

$$SE = \frac{B}{N + L_{cp}} \quad (3.19)$$

3.4 OFDM-IM Performance

The E_b/N_0 curves were generated for OFDM-IM for verification and comparison with classical OFDM. Figures 3.2 and 3.3 show the BER versus E_b/N_0 curves for two implementations of the OFDM-IM schemes using 128 sub-carriers ($N = 128$), with $n = 4$ and $k = 2$. The M-ary modulation schemes utilized for each case are

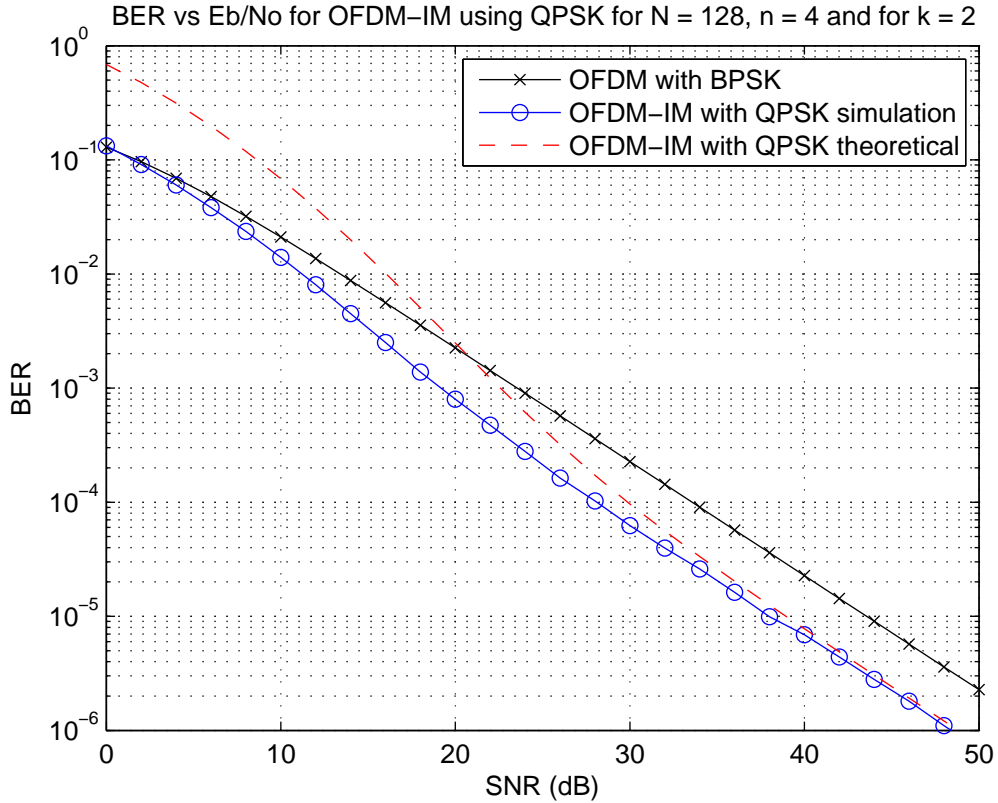


Figure 3.2: BER versus E_b/N_0 for OFDM-IM for $n = 4$ and $k = 2$ using QPSK Quadrature Phase Shift Keying (QPSK) and Binary Phase Shift Keying (BPSK), respectively.

A comparison is also made of the performance of OFDM-IM using $n = 2$ and $k = 4$ for the BPSK and 4-QAM schemes compared to classical OFDM in a 10-tap Rayleigh fading channel ($L_{ch} = 10$ and a cyclic prefix of length $L_{cp} = 11$). As it can be clearly observed in Fig. 3.3, OFDM-IM gives about 5 dB better performance than classical OFDM and that verifies the results in [1]. Furthermore, the simulation results adhere to the loose error bound derived in (28) in [1].

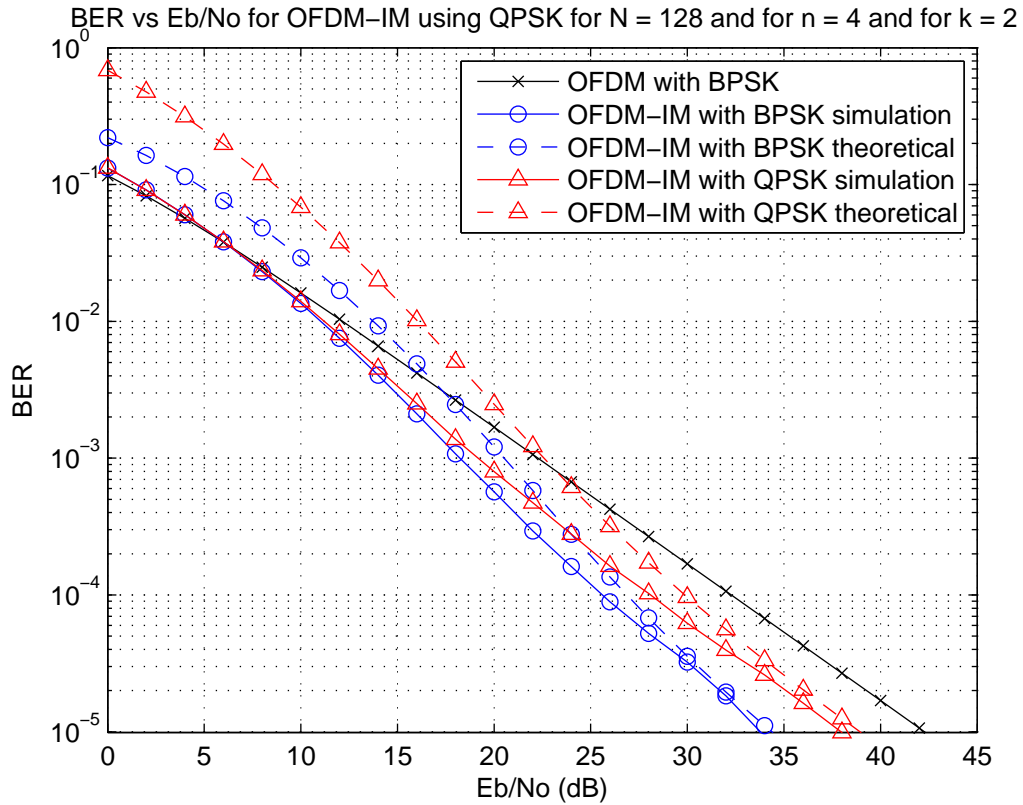


Figure 3.3: Comparison of the BER versus E_b/N_0 for OFDM-IM for $n = 4$ and $k = 2$ using BPSK and QPSK

3.5 Summary

This chapter reviews the concept of OFDM-IM by explaining the transmission model, presenting an example of an OFDM-IM block generation from incoming bit data, and describing the optimum receiver based on the ML criteria. The results confirm that OFDM-IM performs better than classical OFDM in Rayleigh fading channels.

CHAPTER 4

OFDM WITH INDEX SHIFT KEYING

Combining the concept of OFDM with Index Modulation (OFDM-IM) and Generalized Space Shift Keying (GSSK), we suggest a family of modulation techniques that transmit data by switching (a combination of) sub-carriers on and off. In this way, information only transmitted using only the sub-carrier index without any modulated data. The goal is to trade spectral efficiency (SE) for energy efficiency (EE) and a better BER performance. Two new techniques are proposed, OFDM with Generalized Index Shift Keying (OFDM-GISK) and OFDM with Index Shift Keying (OFDM-ISK). The latter represents a special case of OFDM-GISK.

This chapter is organized as follows: In the first section we introduce the OFDM-GISK technique by describing the system model as well as the receiver architecture based on the maximum likelihood method. In sections 4.1 and 4.2, we introduce the framework for OFDM-ISK and OFDM-SBISK including the system

models and the ML receiver architectures. In section 4.3, we derive the analytical expressions for the Average Bit Error Probability (ABEP) and the BER for OFDM-GISK. The analysis is extended to the cases of OFDM-ISK and OFDM-SBISK. Lastly, the simulation results are presented and comparisons are made with classical OFDM and OFDM-IM in terms of BER, SE, EE and complexity.

4.1 OFDM-GISK

In literature, Space Shift Keying (SSK) was proposed before Generalized SSK (GSSK). GSSK is a scheme so that in MIMO systems, only a group of antennas are switched at a time. A similar technique for OFDM would rely on using only one sub-carrier for transmission whereas the general version would utilize a combination of sub-carriers. In this section, we will define the so called OFDM with Generalized Index Shift Keying (OFDM-GISK) first and then present OFDM-ISK as a special case. We begin by presenting the system design of the transmitter.

4.1.1 System Design

Assume an OFDM block with a total number of N sub-carriers. GISK uses n out of these N sub-carriers for transmission which means that n out of N symbols are binary 1's, and the rest are 0's. The complete set of possible realizations for the OFDM block vector \mathbf{x}_F are

$$C_r = C(N, n) \tag{4.1}$$

where the maximum number of bits that can be represented are given by

$$b = \lfloor \log_2(C_r) \rfloor. \quad (4.2)$$

Therefore the number of symbols represented by one block of OFDM-GISK

$$M = 2^b. \quad (4.3)$$

Firstly, we have to determine the indices of the active sub-carriers in OFDM-GISK. For N sub-carriers, we have M different combinations of only n active indices given by

$$\mathbf{I}_\Gamma = [\iota_\Gamma(1) \ \iota_\Gamma(2) \ \dots \ \iota_\Gamma(n)] \quad (4.4)$$

where $\iota_\Gamma(\zeta) \in \{1, \dots, N\}$ for $\zeta = 1, \dots, n$ and $\Gamma \in \{1, \dots, M\}$. The frequency domain OFDM block $\mathbf{x}_\mathbf{F} = [x_F(1) \ x_F(2) \ \dots \ x_F(N)]^T$ such that

$$x_F(\beta) = \begin{cases} 1, & \beta = \iota_\Gamma(\zeta) & \text{for } \beta = 1, \dots, N \\ 0, & \textit{otherwise} & \text{and } \zeta = 1, \dots, n \end{cases} \quad (4.5)$$

Figure 4.1 describes the complete system design of OFDM-GISK.

The average energy of one frame in the frequency domain x_F given by (4.5) is $E[x_F^H X_F] = n$. Classical OFDM transmission techniques are now used starting

with the IFFT to get the time-domain signal

$$\mathbf{x}_T = \frac{N}{\sqrt{n}} \mathcal{F}^{-1}\{\mathbf{x}_F\} = \mathbf{W}_N^H \mathbf{x}_F \quad , \quad (4.6)$$

where the Discrete Fourier Transform (DFT) matrix \mathbf{W}_N is defined such that

$$\mathbf{W}_N^H \mathbf{W}_N = N \mathbf{I}_N, \quad (4.7)$$

and the term $\frac{N}{\sqrt{n}}$ is used to normalize the OFDM time-domain frame energy $E[x_T^H x_T] = N$. At the receiver, a normalization factor of $\frac{\sqrt{n}}{N}$ is employed to recover the OFDM block in the frequency domain.

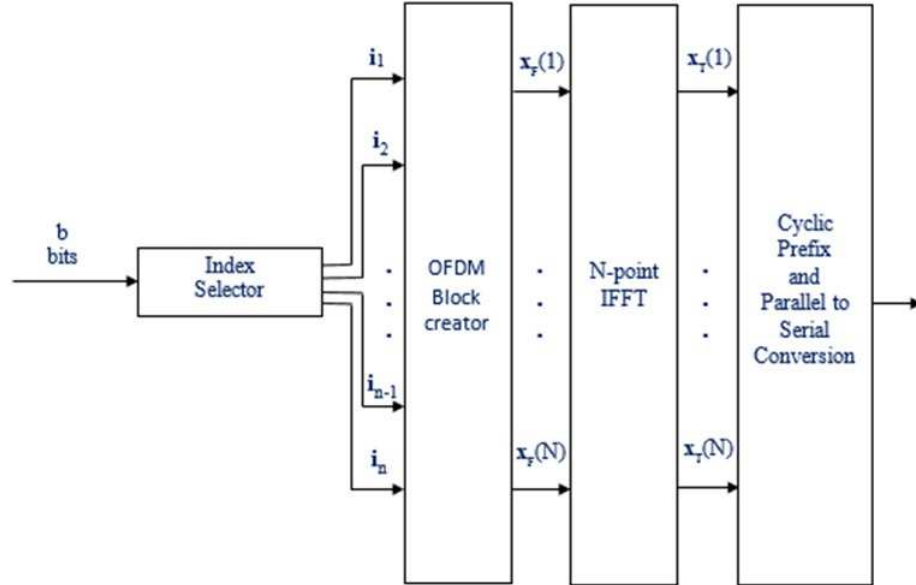


Figure 4.1: Block Diagram of an OFDM-GISK transmission.

4.1.2 ML Receiver implementation

This section defines the maximum likelihood receiver for OFDM-GISK which gives optimum performance. In this chapter, the following assumptions are used. The average energy of each symbol is unity. The channel is modeled as frequency selective slow Rayleigh fading and the noise is zero-mean AWGN. We assume that perfect CSI is available at the receiver.

Received Signal Characterization

Assuming perfect CSI, if the channel consists of L_{ch} taps, then a cyclic prefix of length L_{cp} such that $L_{cp} > L_{ch} + 1$ is appended. The signal is passed through the channel after parallel to serial conversion. The channel can be modeled as frequency selective Rayleigh fading where the coefficients are

$$\mathbf{h}_T = [h_T(1) \ h_T(2) \ \dots \ h_T(L_{ch})]^T, \quad (4.8)$$

such that $h_T(l_{ch}), l_{ch} = 1, \dots, L_{ch}$ are circularly symmetric complex Gaussian Random Variables (RV's) with the following distribution $\mathcal{CN}(0, \frac{1}{L_{ch}})$.

In the case of OFDM for the channel described above, the received signal in the frequency domain can be defined as follows

$$y_F(\beta) = x_F(\beta)h_F(\beta) + w_F(\beta), \quad \beta = 1, \dots, N. \quad (4.9)$$

The received signal $y_F(\beta)$ is an element of the received vector in the frequency domain \mathbf{y}_F . The channel fading coefficients in the frequency domain $h_F(\beta)$ follow the distribution $\mathcal{CN}(0, 1)$ whereas the noise samples $w_F(\beta)$ follows the distribution $\mathcal{CN}(0, \sigma_{0,F}^2)$ where $\sigma_{0,F}^2 = N_{0,F}$.

$N_{0,F}$ is the noise variance in the frequency domain and for OFDM-GISK, it is related to the noise variance in time-domain by

$$N_{0,F} = \frac{n}{N} N_{0,T}. \quad (4.10)$$

The SNR can be defined as $E_b/N_{0,T}$ where the average bit energy $E_b = \frac{(N + L_{cp})}{b}$. The spectral efficiency on the other hand can be defined by $\frac{b}{N + L_{cp}}$ [bits/sec/Hz].

ML Receiver Architecture

As described in section 4.1.1, information is transmitted using a combination of active sub-carriers without any linear modulation. The ML receiver reduces to the detection of the most likely combination of indexes that were active. The search is performed over all possibilities and as one may recall, there are a total of M possibilities. This can be determined by minimizing the following metric:

$$\hat{\mathbf{I}}_\Gamma = \arg \min_{\mathbf{I}_\Gamma} \sum_{\alpha=1}^N |y_F(\alpha) - h_F(\alpha) \tilde{\mathbf{x}}_F(\alpha)|^2, \quad (4.11)$$

where $y_F(\alpha)$ is the received signal and $h_F(\alpha)$ is the corresponding fading coefficient for the α^{th} element of the OFDM block. The vector $\tilde{\mathbf{x}}_F$ represents one possibility

such that

$$\tilde{x}_F(\alpha) = \begin{cases} 1, & \alpha = \iota_\Gamma(\zeta) \\ 0, & \textit{otherwise} \end{cases} \quad (4.12)$$

where $\iota_\Gamma(\zeta) \in \{1, \dots, N\}$ for $\zeta = 1, \dots, n$ and $\Gamma \in \{1, \dots, M\}$.

4.2 OFDM-ISK

Combining concept of OFDM with Index Modulation (OFDM-IM) and Space Shift Keying (SSK), we introduce a new scheme called OFDM with Index Shift Keying (OFDM-ISK). The idea is to transmit information using only the sub-carrier index. We begin by applying the concept of SSK to OFDM where only one sub-carrier is active and the rest are inactive. The data is then passed through the OFDM transmission process.

4.2.1 System Design

Let N denote the number of sub-carriers. In case of OFDM-ISK, $M = N$, where M is the number of symbols. Then the number of bits

$$b = \log_2(M) = \log_2(N) \quad (4.13)$$

For $m = 0, \dots, M - 1$, the $(m + 1)^{th}$ sub-carrier will transmit a binary 1, whereas the rest of the sub-carriers transmit a binary 0. The transmitted vector $\mathbf{x}_F =$

$[x_F(1) \ x_F(2) \ \dots \ x_F(N)]^T$ such that

$$x_F(\beta) = \begin{cases} 0, & \beta \neq m + 1 \\ 1, & \beta = m + 1 \end{cases}. \quad (4.14)$$

Figure 4.2 describes the process of transmission.

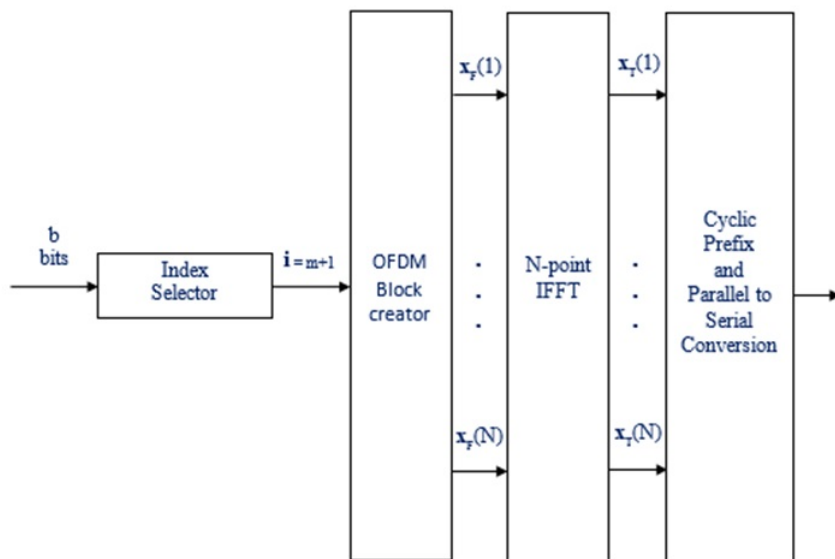


Figure 4.2: Block Diagram of an OFDM-ISK transmission.

4.2.2 ML Receiver implementation

This section describes the received signal and defines the optimum receiver, which is the Maximum Likelihood (ML) receiver for OFDM-ISK. The performance of the ML receiver for OFDM-ISK for various values of N is presented.

Received Signal Characterization

The average energy of one frame in the frequency domain $E[\mathbf{x}_F^H \mathbf{x}_F] = 1$. Classical OFDM is now implemented by applying the Inverse Fast Fourier Transform (IFFT) to get the time-domain signal

$$\mathbf{x}_T = N \mathcal{F}^{-1}\{\mathbf{x}_F\} = \mathbf{W}_N^H \mathbf{x}_F \quad (4.15)$$

where N is the normalization factor in this case and the (DFT) matrix \mathbf{W}_N is as defined in (4.7).

The channel taps in time-domain are as given in (4.8). The taps are iid complex zero-mean Gaussian RV's with variance $\frac{1}{L_{ch}}$, where L_{ch} is the channel length. The received signal vector then takes the same form as the one described by (4.9).

The fading coefficients and the noise samples follow the same distributions as describe in section 4.2.2. The noise variance in time ($N_{0,T}$) and frequency domains ($N_{0,F}$) are related by (4.10) and the relation can be simplified for OFDM-ISK as in (4.16).

$$N_{0,F} = \frac{N_{0,T}}{N} \quad (4.16)$$

The average transmitted energy per bit (E_b) and the spectral efficiency are also as described in section 4.2.2.

ML Receiver Architecture

The ML receiver is basically an exhaustive search over all possibilities for each block of OFDM-ISK. Unlike in OFDM-GISK, since only one index is active at a time, so the ML receiver is simply the most likely index to be active. This can be determined by minimizing the following metric:

$$\hat{\beta} = \arg \min_{\beta} \sum_{m=0}^{M-1} |y_F(\beta) - h_F(\beta)\tilde{x}_F(\beta)|^2 \quad (4.17)$$

where $y_F(j)$ is the received signal and $h_F(j)$ is the corresponding fading coefficient for the j^{th} element of the OFDM block. The vector $\tilde{\mathbf{x}}_F$ represents one possibility such that

$$\tilde{x}_F(j) = \begin{cases} 0, & \beta \neq m + 1 \\ 1, & \beta = m + 1 \end{cases} \quad (4.18)$$

for $m = 0, \dots, M - 1$.

4.3 Performance Evaluation of OFDM-GISK

This section presents the analytical performance of OFDM-GISK. The approach we adopt to derive the analytical BER of the newly defined techniques is similar to the analysis approach in [1]. Although we are using single antenna systems, we can still model the received OFDM block as a Space Time Block Code (STBC). The conditional pairwise error probability (CPEP) is well-known for such a system [51]. The unconditional pairwise error probability can then be obtained by taking

the expectation of the CPEP expression with respect to the channel. The average bit error probability (ABEP) can then be determined by dividing over all possible realizations and the total bits transmitted per block.

An element of the received signal vector \mathbf{y}_F can be described as in (4.9). We represent \mathbf{y}_F as a space-time block code (STBC)

$$\mathbf{y}_F = \mathbf{X}_F \mathbf{h}_F + \mathbf{w}_F, \quad (4.19)$$

by defining \mathbf{X}_F as an $N \times N$ diagonal matrix with $\mathbf{X}_F(\beta, \beta) = x_F(\beta)$ such that

$$\mathbf{X}_F = \begin{bmatrix} x_F(1) & 0 & 0 & \dots & 0 \\ 0 & x_F(2) & 0 & \dots & 0 \\ 0 & 0 & x_F(3) & \dots & 0 \\ \vdots & \vdots & \vdots & \ddots & \vdots \\ 0 & 0 & 0 & \dots & x_F(N) \end{bmatrix}. \quad (4.20)$$

The vectors $\mathbf{h}_F = [h_F(1) h_F(2) \dots h_F(N)]^T$ are the channel coefficients and $\mathbf{w}_F = [w_F(1) w_F(2) \dots w_F(N)]^T$ are the AWGN noise in frequency domain. The transmitted data vector \mathbf{x}_F is modeled as a diagonal matrix instead of the channel \mathbf{h}_F in order to perform a change of variable. The reasons become clear in the following paragraphs. In any case, the conditional pairwise error probability (CPEP) of detecting the wrong sequence $\hat{\mathbf{X}}_F$ when \mathbf{X}_F was transmitted given a

channel \mathbf{h}_F can be defined by [51]

$$P(\mathbf{X}_F \rightarrow \hat{\mathbf{X}}_F | \mathbf{h}_F) = Q \left(\sqrt{\frac{\|(\mathbf{X}_F - \hat{\mathbf{X}}_F) \mathbf{h}_F\|^2}{2N_{0,F}}} \right), \quad (4.21)$$

where $Q(\cdot)$ is the Q-function and $N_{0,F}$ is the noise variance in the frequency domain as described by equation 4.10.

Before trying to solve this CPEP, let us examine the channel more carefully. In particular, the channel in the frequency domain is the N -point FT of \mathbf{h}_T .

$$\mathbf{h}_F = \mathcal{F}\{\mathbf{h}_T\} = \mathbf{W}_N \mathbf{h}_T^0, \quad (4.22)$$

where $\mathbf{h}_T^0 = [\mathbf{h}_T \ \mathbf{0}_{N-L_{CH}}]^T$ is the zero-padded version of the channel in time domain \mathbf{h}_T given by (4.8) and \mathbf{W}_N is the DFT matrix described in (4.7). The channel is no longer independent and it is highly correlated with the correlation matrix

$$\mathbf{R}_{h_F} = \mathbf{W}_N \mathbf{R}_{h_T^0} \mathbf{W}_N^H. \quad (4.23)$$

Since the channel coefficients are i.i.d with variance $\frac{1}{L_{CH}}$ in time-domain, the correlation matrix of the zero-padded version \mathbf{h}_T^0 can be given by

$$\mathbf{R}_{h_T^0} = E[\mathbf{h}_T^0 \mathbf{h}_T^{0H}] = \begin{bmatrix} \frac{1}{L_{CH}} \mathbf{I}_{L_{CH}} & \mathbf{0}_{L_{CH} \times (N-L_{CH})} \\ \mathbf{0}_{(N-L_{CH}) \times L_{CH}} & \mathbf{0}_{(N-L_{CH}) \times (N-L_{CH})} \end{bmatrix}. \quad (4.24)$$

Let us define $\mathbf{D} = (\mathbf{X}_F - \hat{\mathbf{X}}_F)^H (\mathbf{X}_F - \hat{\mathbf{X}}_F)$ and $\delta = \mathbf{h}_F^H \mathbf{D} \mathbf{h}_F$ so that the CPEP can be given by

$$P(\mathbf{X}_F \rightarrow \hat{\mathbf{X}}_F | \mathbf{h}_F) = Q \left(\sqrt{\frac{\delta}{2N_{0,F}}} \right). \quad (4.25)$$

The Q-function can be approximated using the following relation [52]

$$Q(x) \cong \frac{1}{12} \exp \left\{ -\frac{x^2}{2} \right\} + \frac{1}{4} \exp \left\{ -\frac{2x^2}{3} \right\} \quad (4.26)$$

and the unconditional pairwise error probability (UPEP) can be calculated by taking the expectation of the CPEP over \mathbf{h}_F [1, 51, 53, 27, 4].

$$P(\mathbf{X}_F \rightarrow \hat{\mathbf{X}}_F) = E_{\mathbf{h}_F} \left[P(\mathbf{X}_F \rightarrow \hat{\mathbf{X}}_F | \mathbf{h}_F) \right] \quad (4.27)$$

By substituting $\frac{\delta}{2N_{0,F}}$ for x in equation (4.26) and using it to approximate (4.25), the UPEP expression can be obtained by solving the following expectation

$$P(\mathbf{X}_F \rightarrow \hat{\mathbf{X}}_F) = E_{\mathbf{h}_F} \left[\frac{1}{12} \exp \left\{ -\frac{\delta}{4N_{0,F}} \right\} + \frac{1}{4} \exp \left\{ -\frac{\delta}{3N_{0,F}} \right\} \right]. \quad (4.28)$$

This operation reduces to solving the integral of (4.29). Let us define $W_1 = \frac{1}{4N_{0,F}}$ and $W_2 = \frac{1}{3N_{0,F}}$. By using the definition of δ , W_1 and W_2 , we can expand the integral to take the form of (4.30).

$$P(\mathbf{X}_F \rightarrow \hat{\mathbf{X}}_F) = \int_{\mathbf{h}_F} f(\mathbf{h}_F) \left[\frac{1}{12} \exp \left\{ -\frac{\delta}{4N_{0,F}} \right\} + \frac{1}{4} \exp \left\{ -\frac{\delta}{3N_{0,F}} \right\} \right] \quad (4.29)$$

$$= \int_{\mathbf{h}_F} f(\mathbf{h}_F) \left[\frac{1}{12} \exp \{-W_1 \mathbf{h}_F^H \mathbf{D} \mathbf{h}_F\} + \frac{1}{4} \exp \{-W_2 \mathbf{h}_F^H \mathbf{D} \mathbf{h}_F\} \right] d\mathbf{h}_F \quad (4.30)$$

The channel coefficients $\mathbf{h}_F(\beta)$ are circularly symmetric complex normal (\mathcal{CN}) for $\beta = 1, \dots, N$. Then the pdf of \mathbf{h}_F given by $f(\mathbf{h}_F)$ will follow the distribution of a \mathcal{CN} RV. However, it is not easy to determine or to solve the problem using the joint pdf $f(\mathbf{h}_F)$. This integration can be simplified by using the spectral theorem in [54] and the property that for an $n \times 1$ \mathcal{CN} random vector $\mathbf{x} = [x_1, \dots, x_n]$ and an arbitrary complex $n \times n$ matrix \mathbf{A} , \mathbf{z} is also a \mathcal{CN} RV for $\mathbf{z} = \mathbf{A}\mathbf{x}$ [55]. In this case, the pdf of \mathbf{z} is given by

$$f(\mathbf{z}) = \frac{\pi^{-n}}{\det(\mathbf{R}_z)} \exp \{-\mathbf{z}^H \mathbf{R}_z^{-1} \mathbf{z}\}, \quad (4.31)$$

where \mathbf{R}_z is the correlation matrix of \mathbf{z} [55].

We can re-define the frequency domain channel correlation matrix $\mathbf{R}_{h_F} = \mathbf{U} \mathbf{R}_z \mathbf{U}^H$ and the channel vector $\mathbf{h}_F = \mathbf{U} \mathbf{z}$, where $\mathbf{R}_z = E[\mathbf{z} \mathbf{z}^H]$, $r_h = \text{rank}(\mathbf{R}_{h_F})$, $\mathbf{U} \in \mathbb{C}^{N \times r_h}$ and $\mathbf{z} \in \mathbb{C}^{r_h \times 1}$. The new random vector $\mathbf{z} = \mathbf{U}^{-1} \mathbf{h}_F$ has the pdf given by (4.32). By performing a change of variable in (4.30) and substituting (4.32), the UPEP integral can be given by (4.34) and simplified to take the shape of (4.35). This is similar to the form of the UPEP integral for OFDM-IM in (4.25) as given in [1].

$$f(\mathbf{z}) = \frac{\pi^{-r_h}}{\det(\mathbf{R}_z)} \exp \{-\mathbf{z}^H \mathbf{R}_z^{-1} \mathbf{z}\} \quad (4.32)$$

$$P(\mathbf{X}_F \rightarrow \hat{\mathbf{X}}_F) = \int_{\mathbf{z}} f(\mathbf{z}) P(\mathbf{X}_F \rightarrow \hat{\mathbf{X}}_F | \mathbf{z}) \quad (4.33)$$

$$\begin{aligned}
&= \int_{\mathbf{z}} \frac{\pi^{-r_h}}{\det(\mathbf{R}_z)} \exp\{-\mathbf{z}^H \mathbf{R}_z^{-1} \mathbf{z}\} \\
&\quad * \left[\frac{1}{12} \exp\{-W_1 \mathbf{z}^H \mathbf{U}^H \mathbf{D} \mathbf{U} \mathbf{z}\} + \frac{1}{4} \exp\{-W_2 \mathbf{z}^H \mathbf{U}^H \mathbf{D} \mathbf{U} \mathbf{z}\} \right] d\mathbf{z} \quad (4.34)
\end{aligned}$$

$$\begin{aligned}
&= \frac{\pi^{-r_h}}{12 \det(\mathbf{R}_z)} \int_{\mathbf{z}} \exp\{-\mathbf{z}^H [\mathbf{R}_z^{-1} + W_1 \mathbf{U}^H \mathbf{D} \mathbf{U}] \mathbf{z}\} d\mathbf{z} \\
&\quad + \frac{\pi^{-r_h}}{4 \det(\mathbf{R}_z)} \int_{\mathbf{z}} \exp\{-\mathbf{z}^H [\mathbf{R}_z^{-1} + W_2 \mathbf{U}^H \mathbf{D} \mathbf{U}] \mathbf{z}\} d\mathbf{z} \quad (4.35)
\end{aligned}$$

This integral is of the form of [56]

$$\int_{\mathbb{C}^n} \exp\{-\pi^n \mathbf{x}^H \mathbf{A} \mathbf{x}\} d\mathbf{x} = \pi^n \det(\mathbf{A}^{-1}), \quad (4.36)$$

where $\mathbf{A} \in \mathbb{C}^{n \times n}$ and $\mathbf{x} \in \mathbb{C}^{n \times 1}$. We can substitute \mathbf{z} in (4.35) for \mathbf{x} and let $\mathbf{A} = \mathbf{R}_z^{-1} + W_2 \mathbf{U}^H \mathbf{D} \mathbf{U}$. Then using the properties $\det(\mathbf{A}^{-1}) = \frac{1}{\det(\mathbf{A})}$, $\det(\mathbf{A}) \times \det(\mathbf{B}) = \det(\mathbf{A} \times \mathbf{B})$ and $\mathbf{A} \mathbf{A}^{-1} = \mathbf{I}_n$, the UPEP can be given by (4.37). We have the identity $\det(\mathbf{I}_n + \mathbf{N} \mathbf{M}) = \det(\mathbf{I}_m + \mathbf{M} \mathbf{N})$, where \mathbf{N} and \mathbf{M} are $n \times m$ and $m \times n$ matrices, respectively [1]. Using the definition of \mathbf{R}_{h_F} and this identity by substituting r_h for n , N for m , $\mathbf{R}_u \mathbf{U}^H \mathbf{D}$ for \mathbf{N} and \mathbf{U} for \mathbf{M} , the final expression for the UPEP is given by (4.38).

$$P(\mathbf{X}_F \rightarrow \hat{\mathbf{X}}_F) = \frac{1/12}{\det(\mathbf{I}_{r_h} + W_1 \mathbf{R}_z \mathbf{U}^H \mathbf{D} \mathbf{U})} + \frac{1/4}{\det(\mathbf{I}_{r_h} + W_2 \mathbf{R}_z \mathbf{U}^H \mathbf{D} \mathbf{U})} \quad (4.37)$$

$$= \frac{1/12}{\det(\mathbf{I}_N + W_1 \mathbf{R}_{h_F} \mathbf{D})} + \frac{1/4}{\det(\mathbf{I}_N + W_2 \mathbf{R}_{h_F} \mathbf{D})} \quad (4.38)$$

The UPEP expression can be used to calculate the Average Bit Error Probability (ABEP) by averaging over all possibilities of \mathbf{X}_F and the total bits transmitted per block. As one may recall, there can be a total of M possibilities with b bits transmitted for n out of N active sub-carriers. We can re-write the final expression for the UPEP using the definition of \mathbf{D} and $N_{0,F}$ in (4.10) as

$$P(\mathbf{X}_F \rightarrow \hat{\mathbf{X}}_F) = \frac{1/12}{\det \left(\mathbf{I}_N + \frac{N}{4nN_{0,T}} \mathbf{R}_{h_F} \left[\mathbf{X}_F - \hat{\mathbf{X}}_F \right]^H \left[\mathbf{X}_F - \hat{\mathbf{X}}_F \right] \right)} + \frac{1/4}{\det \left(\mathbf{I}_N + \frac{N}{3nN_{0,T}} \mathbf{R}_{h_F} \left[\mathbf{X}_F - \hat{\mathbf{X}}_F \right]^H \left[\mathbf{X}_F - \hat{\mathbf{X}}_F \right] \right)} \quad (4.39)$$

and use it to calculate the ABEP using

$$P_b \leq \frac{1}{b \times M} \sum_1^M \sum_1^{M-1} P(\mathbf{X}_F \rightarrow \hat{\mathbf{X}}_F) e(\mathbf{X}_F, \hat{\mathbf{X}}_F) \quad (4.40)$$

where $e(\mathbf{X}_F, \hat{\mathbf{X}}_F)$ represents the number of bit errors between \mathbf{X}_F and $\hat{\mathbf{X}}_F$.

4.3.1 Extension to OFDM-ISK

If we examine it closely, OFDM-ISK can be described as a special case of OFDM-GISK when the number of active sub-carriers $n = 1$. Mathematically speaking, the received signal model is the same as the one given by (4.9). The CPEP can then be given by (4.21) and the UPEP reduces to solving the expectation in (4.30); the solution is given by (4.38).

We can re-write the UPEP expression using the $N_{0,F}$ definition for OFDM-ISK

given by (4.16).

$$\begin{aligned}
P(\mathbf{X}_{\mathbf{F}} \rightarrow \hat{\mathbf{X}}_{\mathbf{F}}) &= \frac{1/12}{\det \left(\mathbf{I}_N + \frac{N}{4N_{0,T}} \mathbf{R}_{h_{\mathbf{F}}} \left[\mathbf{X}_{\mathbf{F}} - \hat{\mathbf{X}}_{\mathbf{F}} \right]^H \left[\mathbf{X}_{\mathbf{F}} - \hat{\mathbf{X}}_{\mathbf{F}} \right] \right)} \\
&\quad + \frac{1/4}{\det \left(\mathbf{I}_N + \frac{N}{3N_{0,T}} \mathbf{R}_{h_{\mathbf{F}}} \left[\mathbf{X}_{\mathbf{F}} - \hat{\mathbf{X}}_{\mathbf{F}} \right]^H \left[\mathbf{X}_{\mathbf{F}} - \hat{\mathbf{X}}_{\mathbf{F}} \right] \right)} \quad (4.41)
\end{aligned}$$

The UPEP expression can be used to calculate the ABEP as it was done for OFDM-GISK. A total of b bits are transmitted N realizations of $\mathbf{x}_{\mathbf{F}}$ are possible.

The number of errors between each realization is given by $e(\mathbf{X}_{\mathbf{F}}, \hat{\mathbf{X}}_{\mathbf{F}})$.

$$P_b = \frac{1}{b \times N} \sum_1^N \sum_1^{N-1} P(\mathbf{X}_{\mathbf{F}} \rightarrow \hat{\mathbf{X}}_{\mathbf{F}}) e(\mathbf{X}_{\mathbf{F}}, \hat{\mathbf{X}}_{\mathbf{F}}) \quad (4.42)$$

4.4 Results and Discussion

We will now discuss the results of the newly designed techniques and compare analytical and simulation results as well as the performance of OFDM-GISK/ISK against OFDM-IM.

Figure 4.3 illustrates the results for OFDM-ISK for $N = 4$ to $N = 128$ sub-carriers.

The BER performance is clearly improved at the cost of spectral efficiency. It is clear that as the number of sub-carriers is increased, the BER performance declines slightly. In addition, the new scheme is more energy efficient compared to classical OFDM and OFDM-IM. At the same time, the complexity of the ML receiver increases by the power of two, due to the increasing number of possibilities.

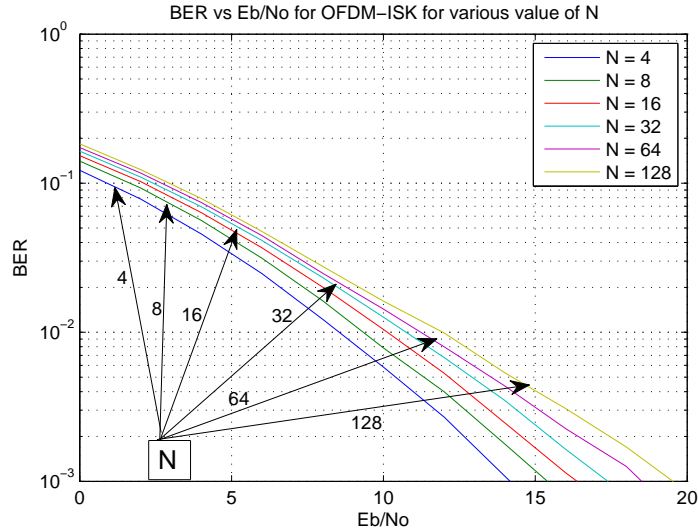


Figure 4.3: BER versus E_b/N_0 OFDM-ISK for various values of N .

To retain the benefits while improving spectral efficiency, we generalize OFDM-ISK to OFDM-GISK.

Figure 4.4 illustrates the results for OFDM-GISK for $N = 8$ with different combinations of n . It is clear that as the number of sub-carriers used is increased, the BER performance declines slightly. In fact, there is no need to go for more than $N/2$ active sub-carriers as the performance decreases without increasing efficiency. The maximum possible combinations occur when $n = N/2$ whereas using $n = 1$ is the same as OFDM-ISK with $N = 8$. OFDM-GISK decreases BER performance and energy efficiency but it improves the spectral efficiency. For example, using OFDM-ISK with 8 sub-carriers allows only the transmission of 3-bits whereas OFDM-GISK can transmit a maximum of 6 bits per block.

Figures 4.5 and 4.6 show the theoretical and simulation plots for OFDM-GISK for a system of 8 sub-carriers. As you can observe, the simulation results match the

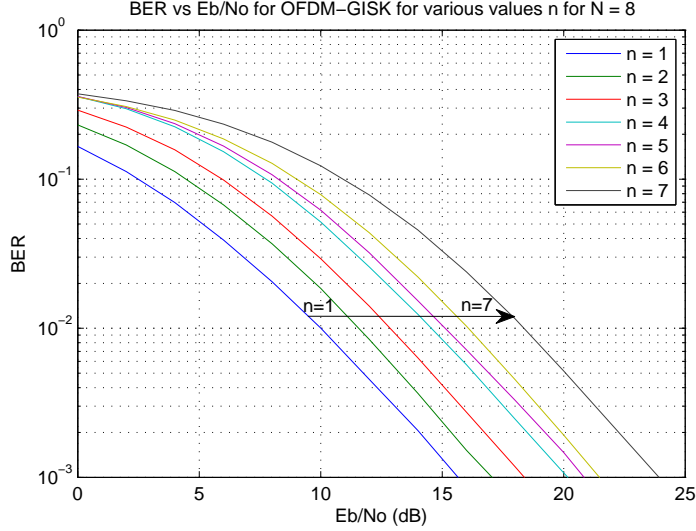


Figure 4.4: BER versus Eb/No OFDM-GISK for $N = 8$ and $n = 1, \dots, 7$.

theoretical results in (4.40) closely. The curves adhere to the loose upper bound, except for at high SNR's. The reason we display only the first four sub-carriers is that using combinations, the maximum realizations are achievable at $n = \frac{N}{2}$. For example using $N - 1$ or 1 sub-carrier will give the same number of possibilities, but a larger n will degrade the performance because the distance between the realizations decreases.

Keeping that in mind, let us study Figure 4.7. Clearly, OFDM-ISK with for $N = 8$ works is the best scheme. The most spectrally efficient configuration with $n = 3$ has a worse performance at low SNR's to begin with, but performs considerably better in the area of interest. For example, at a BER of 10^{-4} , OFDM-ISK provides 5dB better performance than OFDM-IM whereas the $n = 3$ GISK gives a 3dB improvement. This is in the region of SNR between 17 to 22dB. For a BER of 10^{-5} , the improvement is 8dB and 6dB, respectively.

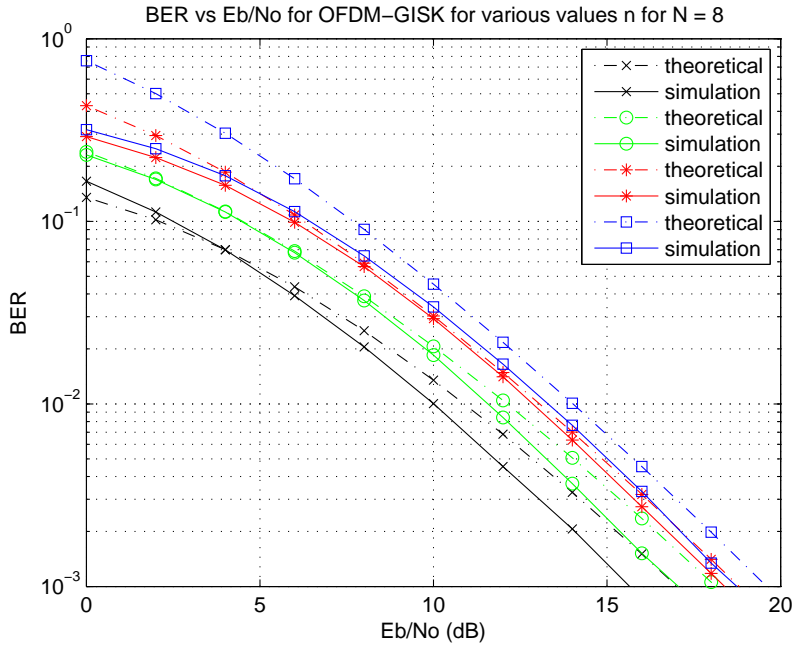


Figure 4.5: Simulation and theoretical results for OFDM-GISK for $N = 8$ and $n = 1, \dots, 4$.

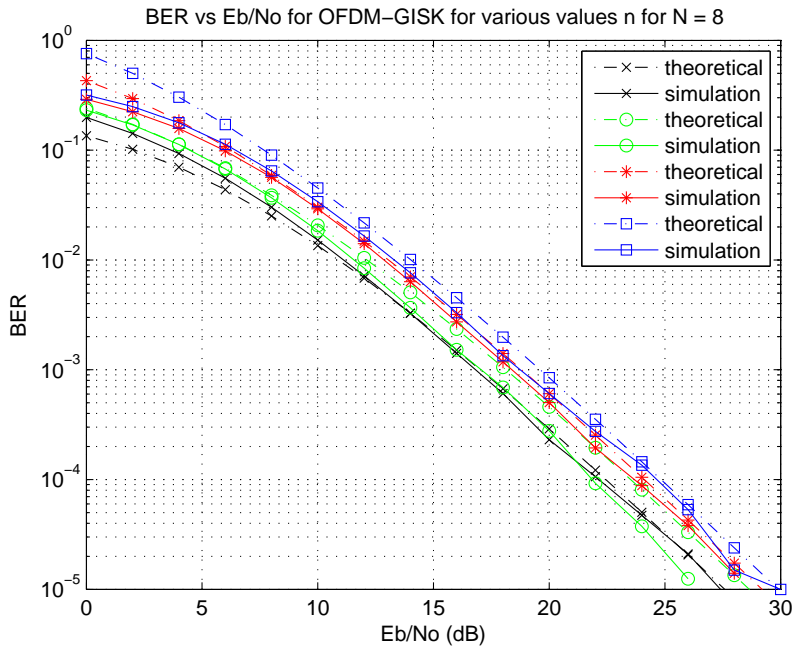


Figure 4.6: Simulation and theoretical results for OFDM-GISK for $N = 8$ and $n = 1, \dots, 4$.

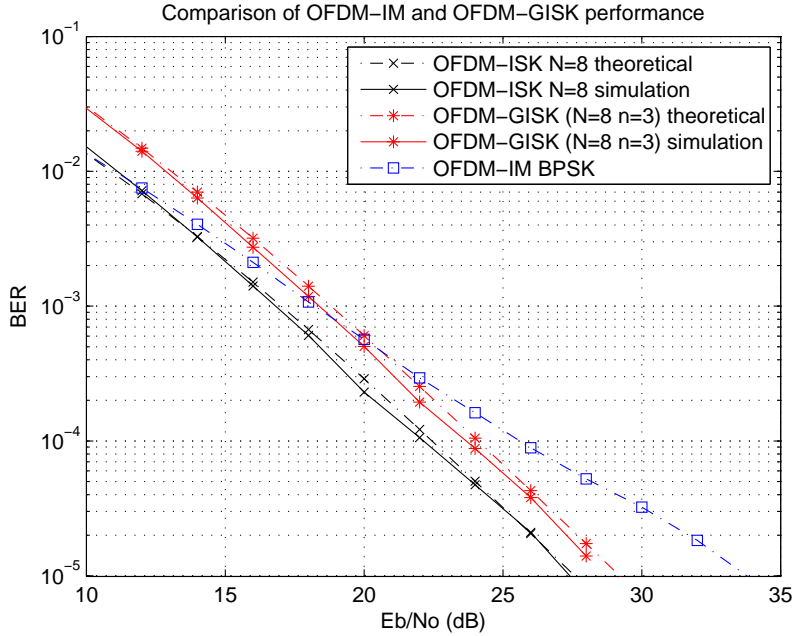


Figure 4.7: Comparison of OFDM-GISK with $N = 8$ and $n = 1$ and 3 versus OFDM-IM.

4.5 Summary

This chapter covers the newly designed ISK techniques by presenting the complete system design, deriving the analytical performance evaluation and comparing the analysis results with the simulations. OFDM-GISK works by simply switching on and off the sub-carriers depending on the incoming data. The detection is performed using the optimum ML receiver. It is shown that as you increase the active sub-carriers, the SE increases but the performance falls. Furthermore, this trade-off can be used to design GISK systems that perform even better than OFDM-IM especially at high SNR's, making this technique suitable for modern technologies such as VLC.

CHAPTER 5

INTERFERENCE: EFFECTS AND MITIGATION

Until now, we have assumed that the channel is ideal; perfect CSI is available. This is not the case in practical applications. It is possible that we may have partial CSI. OFDM transmissions also suffer from interference. Two of the common such impairments are Inter-Carrier Interference (ICI) and Narrow Band Interference (NBI). ICI occurs due to information leaking to adjacent sub-carriers (especially in mobile) whereas NBI occurs due to the occupation of external signals in the transmit frequency band.

One potential application of OFDM-IM is in vehicular networks. Therefore the communication will naturally suffer from ICI. Furthermore, most IEEE wireless standards utilize the (2.4 and 5 GHz) free unlicensed ISM bands. WiFi and BlueTooth technologies use the 2.4 GHz band while WiMax and some WiFi routers occupy the 5GHz band. This can result in unintentional jamming of some of the

transmission bands. NBI can also result from intentional jamming in military applications.

In the literature, the effects of ICI and NBI on OFDM have been studied and various mitigation techniques have been implemented as discussed in section 2.2. The effects of ICI on OFDM-IM and mitigation techniques are evaluated in [1]. To the best of our knowledge, the effects of NBI and cancellation techniques have not yet been evaluated for OFDM-IM. This chapter begins by studying the effects of NBI on OFDM-IM and then proposes a single mitigation method. Lastly, the degradation caused by ICI is evaluated by simulations on the new modulation schemes presented in Chapter 4².

5.1 NBI impairment in OFDM-IM

Narrowband Interference (NBI) is the unintentional or intentional jamming of the sub-carriers in the desired frequency band. For FFT based implementations of OFDM, NBI can be defined as the presence of unwanted signals in less than a quarter of the total sub-carriers. This section describes the NBI model and then evaluates the performance of OFDM-IM and OFDM-ISK in the presence of NBI compared to the classical OFDM.

²Recall that for all schemes \mathbf{x}_F , \mathbf{h}_F , \mathbf{w}_F and \mathbf{y}_F are the $N \times 1$ transmitted, channel, AWGN and received vectors, respectively. Moreover, $\mathbf{y}_F(n) = \mathbf{h}_F(n)\mathbf{x}_F(n) + \mathbf{w}_F(n)$ for $n = 1 \dots N$. Therefore if we define $\mathbf{H}_F = \text{diag}(\mathbf{h}_F)$, then $\mathbf{y}_F = \mathbf{H}_F\mathbf{x}_F + \mathbf{w}_F$. In chapter 5 we will use this model as the starting point and re-define it according to the channel impairments under investigation (NBI or ICI).

5.1.1 NBI Signal Model

The received OFDM signal in time domain can be given by

$$\mathbf{y}_T = \mathbf{h}_T * \mathbf{x}_T + \mathbf{w}_T, \quad (5.1)$$

where \mathbf{h}_T , \mathbf{x}_T and \mathbf{w}_T are the channel impulse response, transmitted frame and the AWGN noise vectors, respectively. Generally speaking, NBI can be modeled as an additive noise component \mathbf{e}_T [16, 17]. The operator $*$ represents the discrete convolution process and can be replaced by using an equivalent toeplitz matrix \mathbf{H}_T , also known as the convolution matrix. Consequently the NBI impaired signal in the time-domain is

$$\mathbf{y}_T = \mathbf{H}_T \mathbf{x}_T + \mathbf{w}_T + \mathbf{e}_T. \quad (5.2)$$

We can re-write (5.2) in terms of the signals in frequency domain to get

$$\mathbf{y}_T = \mathbf{H}_T \mathbf{W}_N^H \mathbf{x}_F + \mathbf{W}_N^H \mathbf{w}_F + \mathbf{W}_N^H \mathbf{e}_F. \quad (5.3)$$

As mentioned, NBI usually is modeled as an additive noise and effects less than $\frac{N}{4}$ sub-carriers [18]. We can model the components of the NBI vector $e_F(i)$ as in the following:

$$\mathbf{e}_F(i) = \begin{cases} g_i, & \alpha \leq i \leq \beta \\ 0, & otherwise \end{cases} \quad (5.4)$$

and the number of affected sub-carriers (or the width of the impairment) w is given by

$$w = \alpha + \beta - 1. \quad (5.5)$$

When the interference is orthogonal, i.e., there is no ICI, the individual components g_i will only effect the i th sub-carrier for $\alpha \leq i \leq \beta$ [16]. In this case, the NBI signal

$$e_i = \sigma_e \sqrt{N} \exp(j\theta), \quad (5.6)$$

where θ is uniformly distributed over $\{-\pi, \pi\}$ ($\theta \sim \mathcal{U}[-\pi, \pi]$) [57]. The interference power is σ_e^2 and here we define the Signal to Narrowband Interference Ratio (SNIR)

$$\frac{E_b}{\sigma_e^2}.$$

5.2 Mitigation using compressed sensing

In this section, we are going to adopt an approach for NBI cancellation using compressive sensing (CS) theory. Gomaa et al. proposed a method to cancel NBI in unfaded OFDM systems by predicting the support using CS [16]. We will modify this approach to predict the support in zero-padded OFDM-IM in fading channels. In this section, we will first give a brief introduction to the subject of compressed sensing, formulate the problem by re-writing (5.2) for zero-padded OFDM-IM and present the modified algorithm.

5.2.1 Compressed Sensing introduction

The objective of CS is to reconstruct a s -sparse vector x of length n from a received signal y and a coefficient matrix ϕ of size $m \times n$. The vector x contains s zero elements or in other words, $n - s$ non-zero elements and $m < n$. If ϕ satisfies the restricted isometric property (RIP) and $m > c_1 s \log \frac{n}{s}$, then x can be estimated reasonably accurately using [58]

$$\hat{\mathbf{x}} = \underset{\text{subject to: } \mathbf{y}=\phi\mathbf{x}}{\arg \min} \|\mathbf{x}\|_{l_1}. \quad (5.7)$$

Similar techniques can be applied to a noisy system such as the one given by

$$\mathbf{y} = \phi\mathbf{x} + \mathbf{w}. \quad (5.8)$$

The received vector $\mathbf{y} \in \mathbb{C}^{m \times 1}$, the transmitted vector $\mathbf{x} \in \mathbb{C}^{N \times 1}$, the measurement matrix $\phi \in \mathbb{C}^{m \times n}$ and the noise vector $\mathbf{w} \in \mathbb{C}^{m \times 1}$. Furthermore, \mathbf{x} is s -sparse, meaning that it has s zeros. In this case, \mathbf{x} can be recovered by solving the following l_1 -minimization

$$\hat{\mathbf{x}} = \arg \min \|\hat{\mathbf{x}}\|_{l_1} \quad \text{subject to:} \quad \|\mathbf{y} - \phi\mathbf{x}\|_2 \leq \eta. \quad (5.9)$$

This is in fact a convex optimization problem in the standard form of

$$\text{minimize } \mathbf{f}^T \mathbf{x} \quad \text{subject to:} \quad \|\mathbf{A}\mathbf{x} + \mathbf{b}\|_2 \leq \mathbf{c}\mathbf{x} + \mathbf{d} \quad (5.10)$$

and it can be solved efficiently using a second order cone program [59]. Please note that an l_1 norm can be expressed as a matrix multiplication described by the following

$$\|\mathbf{x}\| = \mathbf{o}^T \mathbf{x} \quad \text{for} \quad \mathbf{o} = [1 \dots 1]^T \quad \text{and} \quad \mathbf{o}, \mathbf{x} \in \mathbb{C}^n. \quad (5.11)$$

5.2.2 OFDM-IM with zero padding

As described in (5.2), the received signal can be written as a toeplitz matrix multiplication. For the zero-padding case, we can the received signal with the guard band in TD as [13]

$$\mathbf{y}_T = \mathbf{H}_T \mathbf{x}_T + \mathbf{W}_L^H \mathbf{e}_F + \mathbf{w}_T. \quad (5.12)$$

Please note that in this model, the received, NBI support and noise vectors are $(N + L_{cp}) \times 1$. The transmitted vector \mathbf{x}_T is $N \times 1$ whereas the modified channel matrix \mathbf{H}_T is $(N + L_{cp}) \times N$. \mathbf{W}_L is the $(N + L_{cp}) \times (N + L_{cp})$ DFT matrix. The variable L_{cp} now represents the length of the zero-padding and the assumption $L_{cp} \geq L_{ch} - 1$ holds. The NBI support vector \mathbf{e}_F is sparse and the current system of equations can be solved using CS techniques.

However, first it is important to remove the unknown transmitted sequence \mathbf{x}_T in order to make the system in the form of (5.8). In order to achieve this, we need to design a matrix \mathbf{F} such that $\mathbf{F}\mathbf{H}_T = 0$. Actually, the structure of the channel

matrix given in (5.13) makes this process efficient.

$$\mathbf{H}_T = \begin{bmatrix} \mathbf{H}_Z \\ \mathbf{0}_{L_{cp}-L_{ch}+1 \times N} \end{bmatrix}. \quad (5.13)$$

The toeplitz $(N + L_{ch} - 1) \times N$ channel matrix is represented by \mathbf{H}_Z followed by $(L_{cp} - L_{ch} + 1)$ rows of zeros.

5.2.3 Zero Forcing matrix

Once we have a matrix \mathbf{H}_T in the form of (5.13), the zero forcing matrix can then be designed as $\mathbf{F} = [\mathbf{F}_Z \quad \mathbf{F}_N]$. We can design \mathbf{F}_Z by solving the system $\mathbf{F}_Z \mathbf{H}_Z = 0$. The solution is typically given by [16]

$$\mathbf{F}_Z = \mathbf{I}_{N+L_{ch}-1} - \mathbf{H}_Z \mathbf{H}_Z^\dagger, \quad (5.14)$$

where \mathbf{H}_Z^\dagger represents the pseudoinverse such that

$$\mathbf{H}_Z^\dagger = (\mathbf{H}_Z^H \mathbf{H}_Z)^{-1} \mathbf{H}_Z^H. \quad (5.15)$$

Although this approach is sufficient to obtain the expression given by (5.12) in the form of (5.8), the calculation requires computation of the inverse of large matrices. Goma et al. proposed a more efficient approach exploiting the structure of \mathbf{H}_Z [16]. They perform a QR factorization of \mathbf{H}_Z such that $\mathbf{H}_Z = \mathbf{Q}\mathbf{R}$ where $\mathbf{Q} = [\mathbf{Q}_1 \quad \mathbf{Q}_2]$ and \mathbf{Q}_1 is an $(N + L_{ch} - 1) \times N$ matrix. After some manipulations

it is shown that

$$\mathbf{H}_Z = \mathbf{I}_{N+L_{ch}-1} - \mathbf{Q}_1 \mathbf{Q}_1^H. \quad (5.16)$$

5.2.4 Modified CS based approach

Once we have the matrix that can cancel the transmitted vector, the system can be re-written as follows:

$$\bar{\mathbf{y}}_T = \mathbf{F} \mathbf{y}_T = \mathbf{F} \mathbf{H}_T \mathbf{x}_T + \mathbf{F} \mathbf{W}_L^H \mathbf{e}_F + \mathbf{F} \mathbf{w}_T. \quad (5.17)$$

Let $\mathbf{A} = \mathbf{F} \mathbf{W}_L^H$, $\mathbf{w}_Z = \mathbf{F} \mathbf{w}_T$ and recall that $\mathbf{F} \mathbf{H}_T = 0$. In order to match the form of (5.8), this result can be re-written as .

$$\bar{\mathbf{y}}_T = \mathbf{A} \mathbf{e}_F + \mathbf{w}_Z. \quad (5.18)$$

We can now formulate the recovery process of the indexes of the NBI affected sub-carriers as a convex optimization problem given by

$$\hat{\mathbf{e}}_F = \min_{\hat{\mathbf{e}}_F \in \mathbb{C}^{N+L_{cp}}} \|\hat{\mathbf{e}}_F\|_1 \quad \text{subject to:} \quad \|\bar{\mathbf{y}} - \mathbf{A} \hat{\mathbf{e}}_F\|_2 \leq \eta. \quad (5.19)$$

Recall that $\mathbf{F} = [\mathbf{F}_Z \quad \mathbf{F}_N]$ where \mathbf{F}_Z can be obtained from (5.14). The choice of the contents of \mathbf{F}_N can be done arbitrarily. However, the recovery process can be made robust by using a zero-mean Gaussian distribution with variance $1/\nu$, where ν represents the number non-zero elements, or in our case the number of

jammed sub-carriers [60, 61].

The claim of the original algorithm designers was that it is completely blind recovery. However, a guess of the NBI support is needed and as more than 5 elements do not effect the performance (as will be shown in 5.3), an estimate of $\nu = 5$ works well. Furthermore, the error term η has to be selected such that it bounds the noise power. A guideline can be followed to set the value of η based on (6.5) in [62].

The system can now be solved using convex optimization. In fact, it is a second order cone program that can be solved using off-the-shelf solvers [59]. We used CVX, a program for defining and obtaining the solutions of convex programs, to solve (5.19) [63, 64]. The solution will be the estimated jammer locations \hat{j} and the corresponding values g_j where $\hat{\mathbf{e}}_F(\hat{j}) = g_j$.

Once the NBI support vector has been obtained, we apply our modified approach to reconstruct the received signal vector without the zero padded prefix. The received signal in time can be reconstructed using

$$\hat{\mathbf{y}}_T = \mathbf{y}_T - \mathbf{W}_L^H \hat{\mathbf{e}}_F. \quad (5.20)$$

The reconstructed signal can be obtained by adding the guard band to the first L_{cp} elements of the reconstructed vector and discarding the last L_{cp} elements. The

operation can be described by as a matrix multiplication given by

$$\tilde{\mathbf{y}}_T = \begin{bmatrix} \mathbf{I}_N & \mathbf{I}_{L_{cp}} \\ \mathbf{0}_{L_{cp} \times N} & \mathbf{0}_{N \times L_{cp}} \end{bmatrix} \hat{\mathbf{y}}_T \quad (5.21)$$

For classical OFDM, the next step is to apply a linear detector such as the MMSE. However, we apply the optimum ML detector given by (3.16). The algorithm is summarized below.

Algorithm summary

1. Compute \mathbf{F}_Z using (5.14).
2. Formulate the convex optimization problem in (5.19) by multiplying $\bar{\mathbf{y}}_T$ with \mathbf{F}_Z .
3. Solve the program in (5.19).
4. Reconstruct the received signal in TD with the guard band using (5.20).
5. Remove the guard band using (5.21).
6. Reconstruct the OFDM-IM frame from $\tilde{\mathbf{y}}_T$ using the ML receiver described by (3.16).

5.3 NBI simulation results and analysis

Based on the model given in section 5.1.1, we simulate the effects of NBI on OFDM-IM and the designed OFDM-GISK techniques. The NBI signal can be of

various width w and take a range of SNIR values for a wireless system working at a certain SNR. We first investigate the impact of the jammer width and SNIR. Then we study the performance degradation for NBI support affecting a specific number of sub-carriers with a particular SNIR.

5.3.1 Impact of jammer width w

Previous studies of NBI impairments in classical OFDM systems [16, 19] show that for particular SNIR values. In this part, we examine if varying the number of affected sub-carriers will have any impact on IM techniques.

Figure 5.1 illustrates how the performance degradation of both OFDM and OFDM-IM in the presence of NBI of various widths. We evaluate the system at a practical SNR value of 15dB for wireless systems and under high and low interference powers; SNIR's of -10 and +10dB. At an SNIR of -10dB, changing the jammer widths a negligible effect for OFDM as already shown by [16]. In contrast, the performance of OFDM-IM suffers sharply as the number of jammers are increased from 1 to 6. For larger tones, the performance degrades by a small amount.

In case of weak interferer's, there is a more pronounced impact on OFDM as expected. However, OFDM-IM is better able to stand the impact low power impairments where the performance degrades linearly. However, as you can see from Figure 5.2, at higher SNR's the slope of the BER curve is larger hinting at a limit to IM's ability to withstand NBI. Similarly for the case of high interference power,

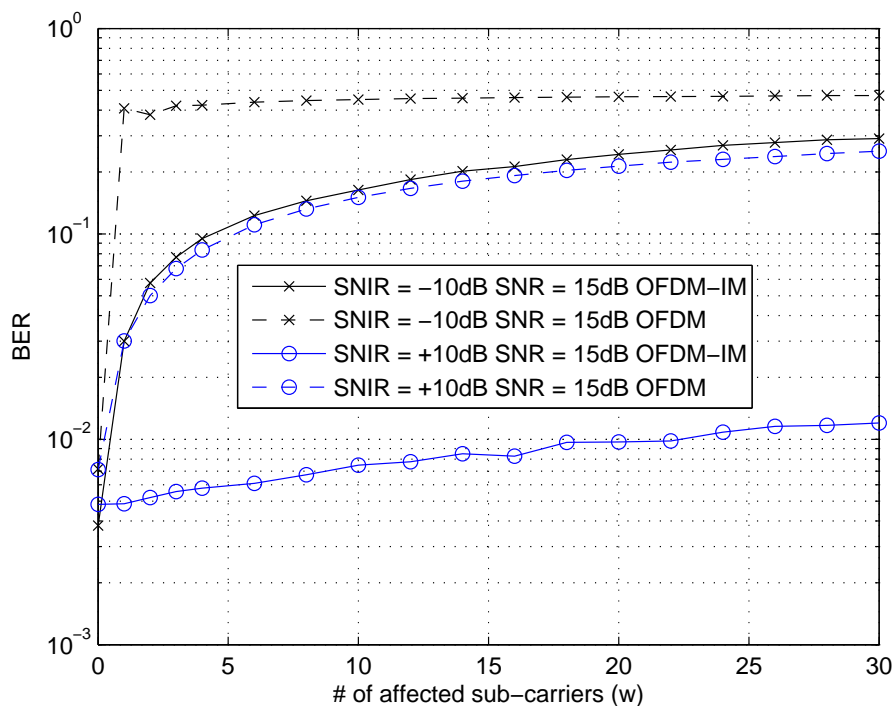


Figure 5.1: BER versus w for OFDM and OFDM-IM for $E_b/N_o = 15dB$

the performance declines sharply for the first few jammers and then reaches an error floor. As we will show later, OFDM-IM is quite resilient to the effects of NBI at low SNR.

5.3.2 Impact of Interference Power

We have discussed that for high levels of interference, increasing the number of jammers only effects the performance for low number of NBI elements (between 1 to 5). In this section, we will again evaluate the performance of IM techniques by simulation, but this time against the SNIR for small number of interferers. We will examine the behavior of the BER curves over a range of SNIR of -20 to 20dB

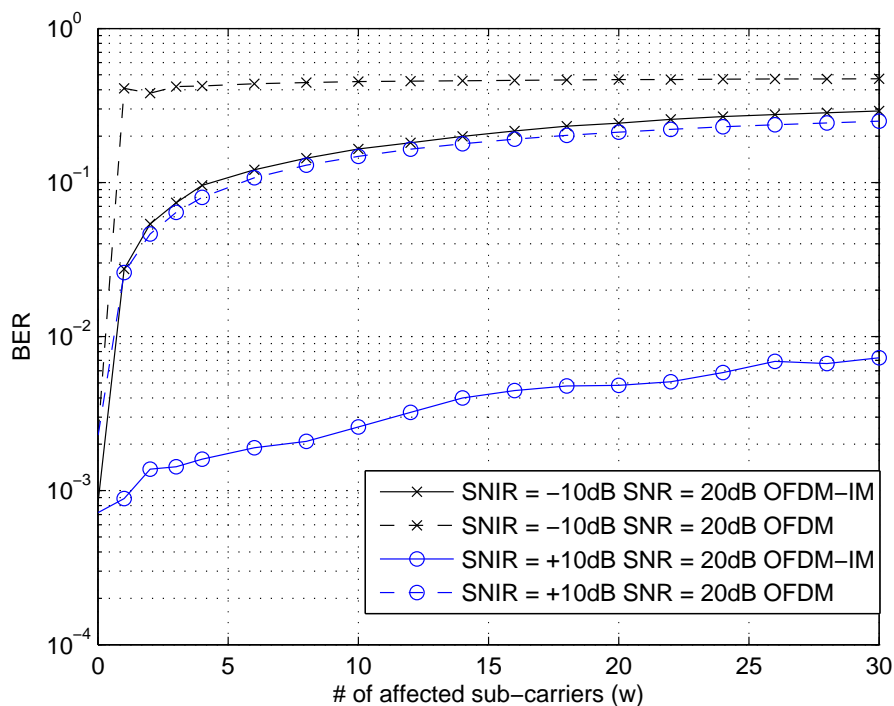


Figure 5.2: BER versus w for OFDM and OFDM-IM for $E_b/N_o = 15dB$

for the cases of one and three jammed sub-carriers.

As you can observe in both, Figures 5.3 and 5.4, as the SNIR is increased from -10 to +10dB, there is negligible improvement in the performance of classical OFDM transmission. In contrast, as the jamming power is reduced, OFDM-IM is able to improve its performance considerably up to a certain SNIR. For very high or very low jamming powers ($SNIR < -10dB$ or $SNIR > 15dB$) the system has an error floor. For practical purposes, this is significant because NBI, whether intentional or unintentional, even from high power sources would fall within this range. This means that even at an SNIR of -10dB from one source, the system

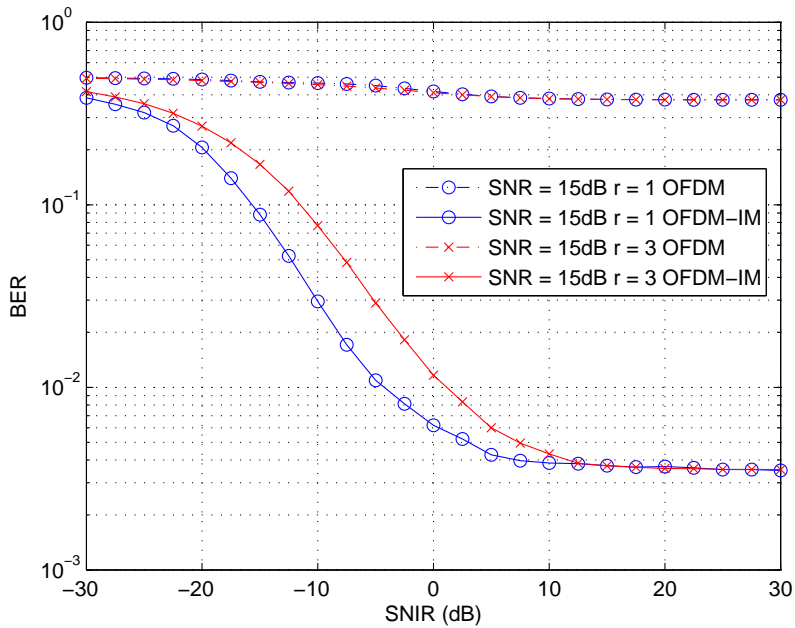


Figure 5.3: BER versus SNIR of OFDM and OFDM-IM in presence of 1 and 3 jammers at an SNR of 15dB.

can function reasonably.

Furthermore, the number of NBI components have an impact on the performance of OFDM-IM and we showed before that this is the case for a low number of jammers. For classical OFDM, this is not significant unless the NBI ratio is extremely low (below 20dB). As illustrated in Fig. 5.5, OFDM-IM performs better by about 4dB with respect to the SNIR at a BER of 10^{-2} and at an SNR of 15dB if there is only one NBI source compared to three. At a system working on a higher SNR of 20dB, the same improvement is offered but at a higher BER of 10^{-3} .

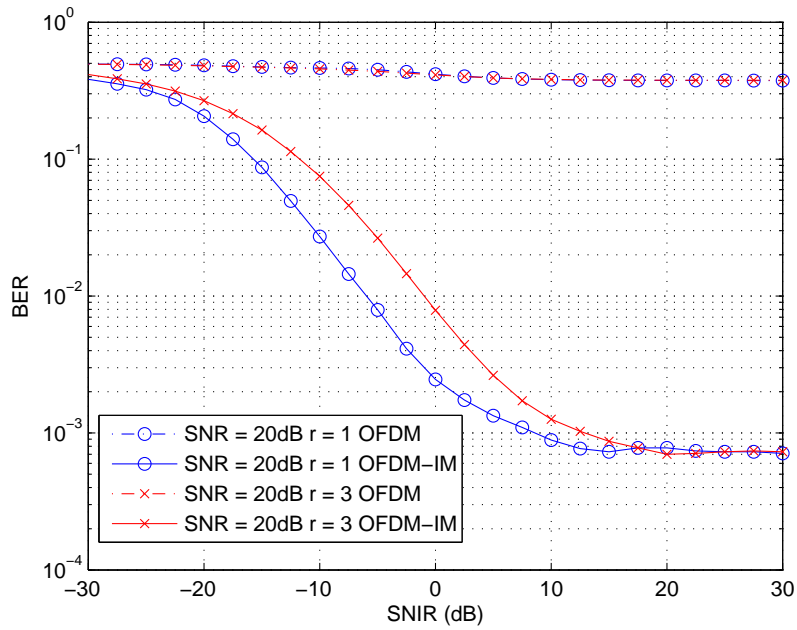


Figure 5.4: BER versus SNIR of OFDM and OFDM-IM in presence of 1 and 3 jammers at an SNR of 20dB.

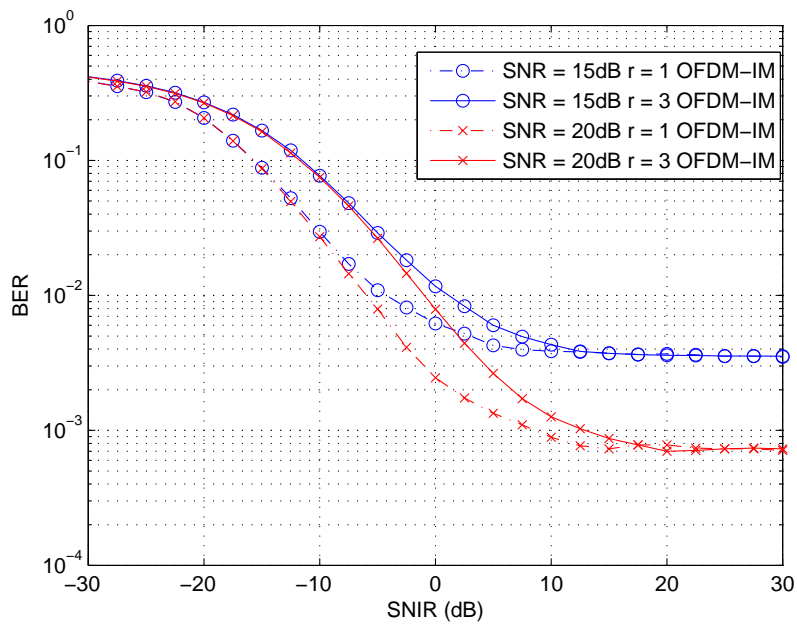


Figure 5.5: BER versus SNIR of OFDM and OFDM-IM in presence of one and three jammers at an SNR's of 15 and 20 dB.

5.3.3 Performance degradation in OFDM-IM

In this section, we evaluate the degradation in error rate of OFDM-IM. As described previously, the performance is not affected a lot by increasing the number of jammed sub-carriers for $w > 5$. So for comparison purposes we will continue to take the cases of 1 and 3 jammers. The performance is then studied for the cases of low and high σ_e^2 .

As it can be seen from Figures 5.6 and 5.7, classical OFDM techniques fail in the presence of NBI regardless of the jammer width w . This observation matches the results of [16, 17] and also our own observation in Section 5.3.1. By comparison, OFDM-IM is quite resilient to NBI and at an SNIR of -10dB offers BER of about 10^{-2} . For low NBI powers, OFDM-IM performs quite well and does not reach an error floor until after an SNR of 30dB.

Practically speaking, mitigation methods will not be needed for most wireless applications as they operate at SNR's between 15-25dB. Moreover, the number of NBI sources has a slight inverse effect on the performance at SNR's above 20dB when the SNIR is high. For higher jamming powers, the number of sources does not have much of an impact.

5.3.4 NBI Mitigation Results

As we have observed from the previous sections, OFDM-IM has the capability to withstand the impact of NBI for SNIR's up to -10 dB. However, at very high jamming powers, even OFDM-IM performance is degraded. The modified CS-ML

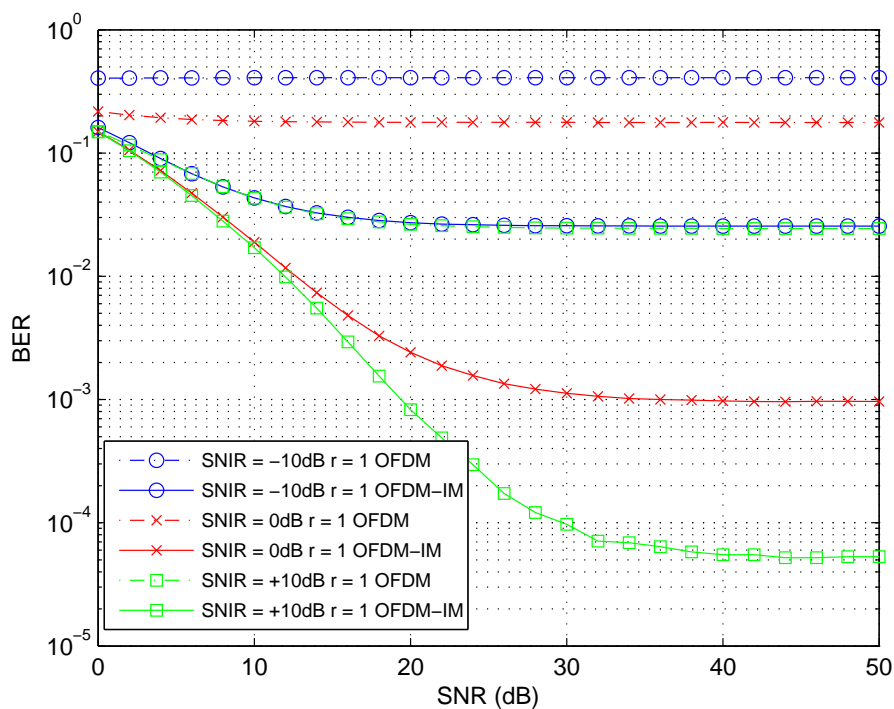


Figure 5.6: Performance of OFDM and OFDM-IM in presence of one jammer.

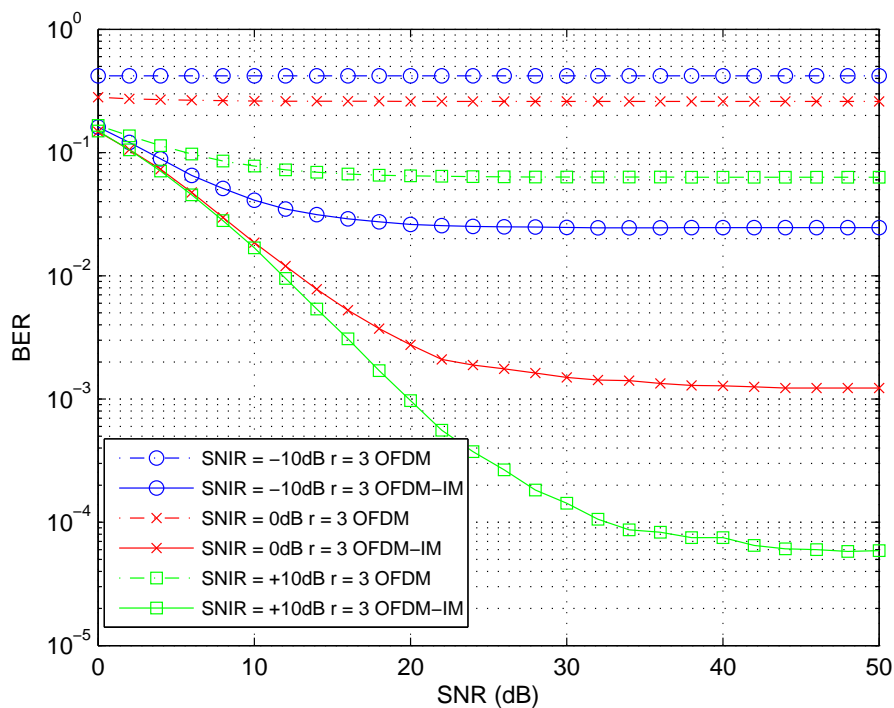


Figure 5.7: Performance of OFDM and OFDM-IM in presence of three jammers.

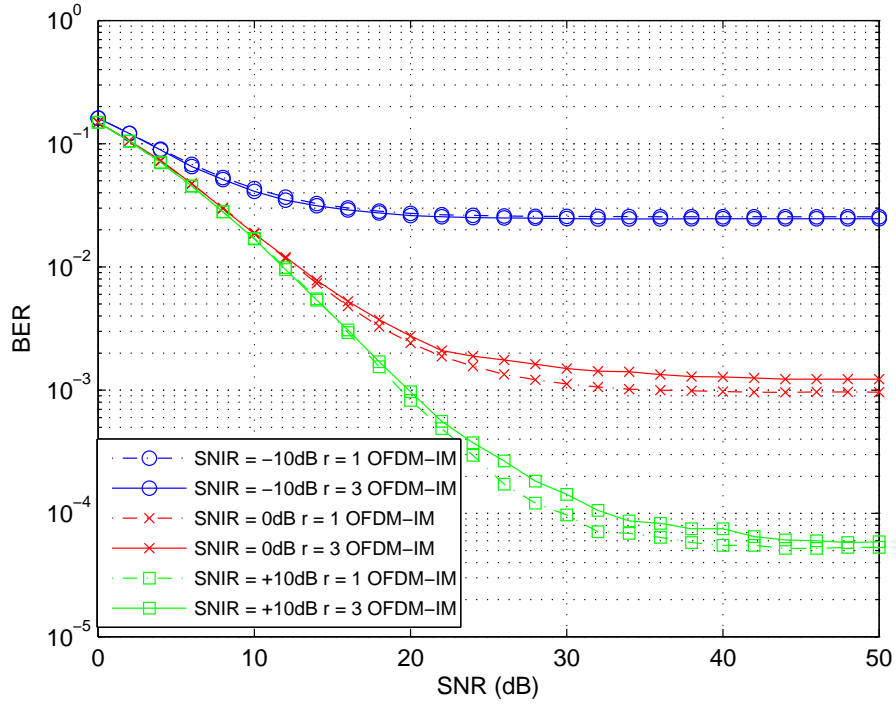


Figure 5.8: Performance of OFDM and OFDM-IM in presence of 3 jammers

approach developed in Section 5.2 with zero padding is applied to OFDM-IM suffering from 3 jamming sources at SNIR values of -15 and -20dB. The performance is improved and the results are similar to [16] for classical OFDM.

In the unmitigated case, OFDM-IM can barely achieve a BER of 10^{-1} at an interference ratio of -15dB and below 10^{-1} in the case of -20dB. However, Figure 5.9 confirms that after the cancellation scheme is applied, the system performs close to case of no NBI. Only at SNR's of greater than 20dB does the system reach an error floor (10^{-3} in the case of -20dB and between 10^{-3} and 10^{-4} in the case of -15dB). In the region of interest (10-20 dB), the cancellation algorithm is able to improve the performance significantly.

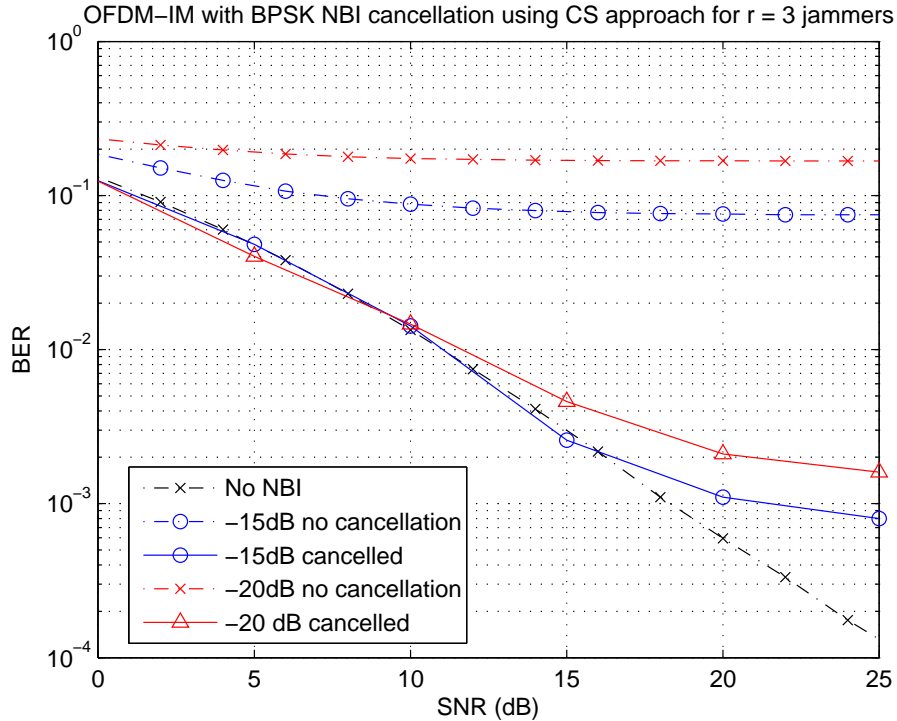


Figure 5.9: Performance of OFDM-IM in presence of 3 jammers after cancellation for an SNIR of -15dB

5.4 Review of ICI in OFDM-IM

In frequency-selective channels, OFDM eliminates inter-symbol interference (ISI) and a one-tap equalizer is sufficient [65]. In fast fading channels resulting from high mobility applications such as vehicular networks, the channels are no longer orthogonal which leads to ICI. Consequently, the transmitted signal is also affected by the channel response at the other sub-carriers. In the following subsections, we described the OFDM-IM signal model in ICI, review a few detection schemes and their performance.

5.4.1 Signal Model

The received signal in time domain can be expressed as [66]

$$y_F(i) = H_T(i)x_F(i) + \sum_{\substack{\hat{i}=0 \\ \hat{i} \neq i}}^{N-1} \left(\sum_{l=0}^{L_{ch}-1} H_T[l, i - \hat{i}] e^{-\frac{2\pi}{N} l \hat{i}} \right) + w_F(i) \quad (5.22)$$

where \mathbf{H}_T is the equivalent time-domain channel matrix such that

$$\mathbf{H}_T = [\mathbf{h}_T(0) \dots \mathbf{h}_T(N-1)], \quad (5.23)$$

where $\mathbf{h}_T(j)$ is the channel impulse response cyclic shifted downwards by $j+1$ elements [65]. In the frequency domain, we can represent this system using an equivalent channel \mathbf{V}_F given by [65, 8]:

$$\mathbf{V}_F = \mathbf{W}_N \mathbf{H}_T \mathbf{W}_N^H. \quad (5.24)$$

The received signal vector then becomes

$$\mathbf{y}_F = \mathbf{V}_F \mathbf{x}_F + \mathbf{w}_F, \quad (5.25)$$

where \mathbf{V}_F is no longer diagonal.

Usually, in highly mobile environments the OFDM frame is padded with zeros (excluding the cyclic prefix) in order to prevent inter-block interference. In our case, we will assume that the first and last L_z elements are zeros (a total of $2L_z$).

So the actual received signal is

$$\bar{\mathbf{y}}_F = \bar{\mathbf{V}}_F \bar{\mathbf{x}}_F + \bar{\mathbf{w}}_F, \quad (5.26)$$

where $\bar{\mathbf{y}}_F = \mathbf{y}_F(\lambda)$, $\bar{\mathbf{x}}_F = \mathbf{x}_F(\lambda)$, $\bar{\mathbf{w}}_F = \mathbf{w}_F(\lambda)$ and $\bar{\mathbf{V}}_F = \mathbf{V}_F(\lambda, \lambda)$ for $\lambda = L_z + 1 : N - L_z$. The authors of [1] proposed four detectors: one linear detector based on the MMSE criteria and three detectors that exploit the structure of the transmitted OFDM-IM frame \mathbf{x}_F .

5.4.2 ICI cancellation schemes for OFDM-IM

The MMSE equalizer treats ICI in OFDM systems similar to the ISI in single-carrier systems. An equalizer based on this criteria is readily available in literature [65, 66]. The estimated received signal after ICI is

$$\hat{\mathbf{y}}_F = \bar{\mathbf{V}}_F^H \left[\bar{\mathbf{V}}_F \bar{\mathbf{V}}_F^H + \frac{\mathbf{I}_{N_{\text{sub}}}}{\rho_F} \right]^{-1} \bar{\mathbf{y}}_F. \quad (5.27)$$

N_{sub} is the number of used sub-carriers $N - 2L_z$ and ρ_F is the equivalent SNR in the frequency domain. The ML detector described by (3.16) can be applied to $\hat{\mathbf{y}}_F$.

The next detection scheme is the interference unaware sub-matrix detector that

uses the assumption $\mathbf{V}_F \approx \hat{\mathbf{V}}_F$ such that

$$\hat{\mathbf{V}}_F = \begin{bmatrix} \bar{\mathbf{V}}_{F,1} & 0 & \dots & 0 \\ 0 & \bar{\mathbf{V}}_{F,2} & \dots & 0 \\ \vdots & \vdots & \ddots & \vdots \\ 0 & 0 & \dots & \bar{\mathbf{V}}_{F,G} \end{bmatrix}, \quad (5.28)$$

where $\bar{\mathbf{V}}_{F,g} = \mathbf{V}_F(g[n-1] + 1 : gn, g[n-1] + 1 : gn)$. A detector similar to the ML receiver is applied by minimized the following metric

$$\hat{\mathbf{x}}_F^g = \arg \min_{\bar{\mathbf{x}}_F^g} \|\bar{\mathbf{y}}_F^g - \hat{\mathbf{V}}_{F,g} \bar{\mathbf{x}}_F^g\|^2 \quad (5.29)$$

where $\bar{\mathbf{y}}_F^g$ and $\bar{\mathbf{x}}_F^g$ are $\bar{\mathbf{y}}(g[n-1] + 1 : gn)$ and $\bar{\mathbf{x}}(g[n-1] + 1 : gn)$, respectively.

The detector is highly complex as the $\bar{\mathbf{x}}_F^g$ already has cM^k realizations.

An improved version of the submatrix detector is the block cancellation (BC) detector. After each iteration g , the detector updates the elements of $\bar{\mathbf{y}}_F^g$ as shown in (5.30) with the assumption that $\hat{\mathbf{x}}_F^g = \mathbf{x}_F^g$ and $\tilde{\mathbf{V}}_F^g = \hat{\mathbf{V}}_F(1 : N_{sub}, g[n-1] + 1 : gn)$.

$$\bar{\mathbf{y}}_F = \bar{\mathbf{y}}_F - \tilde{\mathbf{V}}_F^g \hat{\mathbf{x}}_F^g \quad (5.30)$$

The most sophisticated receiver is the signal power (SP) detector which applies the BC scheme after sorting $\bar{\mathbf{V}}_F^g$ in $\hat{\mathbf{V}}_F$ according to their signal powers SP_g , which

are defined for each sub-block as

$$SP_g = \|\bar{\mathbf{V}}_F^g\|_F^2. \quad (5.31)$$

5.4.3 Performance of various ICI cancellation schemes for OFDM-IM

Figure 5.10 shows the performance of the detection schemes for a system employing $N = 128$ sub-carriers with $n = 4$ and $k = 2$. A total of the first $L_z = 20$ carriers are padded with zeros. The performance of all four proposed detection schemes in Section 5.4.2 are compared against the scenario where there is no ICI and the case when no cancellation scheme is employed.

The MMSE detector performs worse the case of no cancellation in the region of low SNR. However, at higher SNR's the performance improves and reaches the error floors achieved by the submatrix and block cancellation (BC) detectors. Note that this behavior is in contrast to the case of classical OFDM where the linear Zero Forcing (ZF) and MMSE detectors reach an error floor. In addition, it initially degrades the performance because one characteristic of IM techniques is that the sub-carrier positions carry information. By canceling the effect of the ICI, we also inadvertently end up removing the diversity gained through the channel.

The interference unaware sub-matrix detector improves the performance in the region of $SNR \leq 20\text{dB}$ as illustrated in Figure 5.10. However, it reaches an error floor of about 10^{-3} . As expected, the BC detector improves on that statistic and

it almost achieves a floor of about 10^{-4} at about 25dB. Although updating the received signal based on the estimates of the detected symbols helps, it has its limits because the result of an erroneous prediction may propagate for several sub-blocks before being nullified. In contrast, the SP detector performs like the unimpaired signal up-to an SNR of 35dB. This is because by sorting according to the signal powers, we maximize the probability of getting the earliest predictions right.

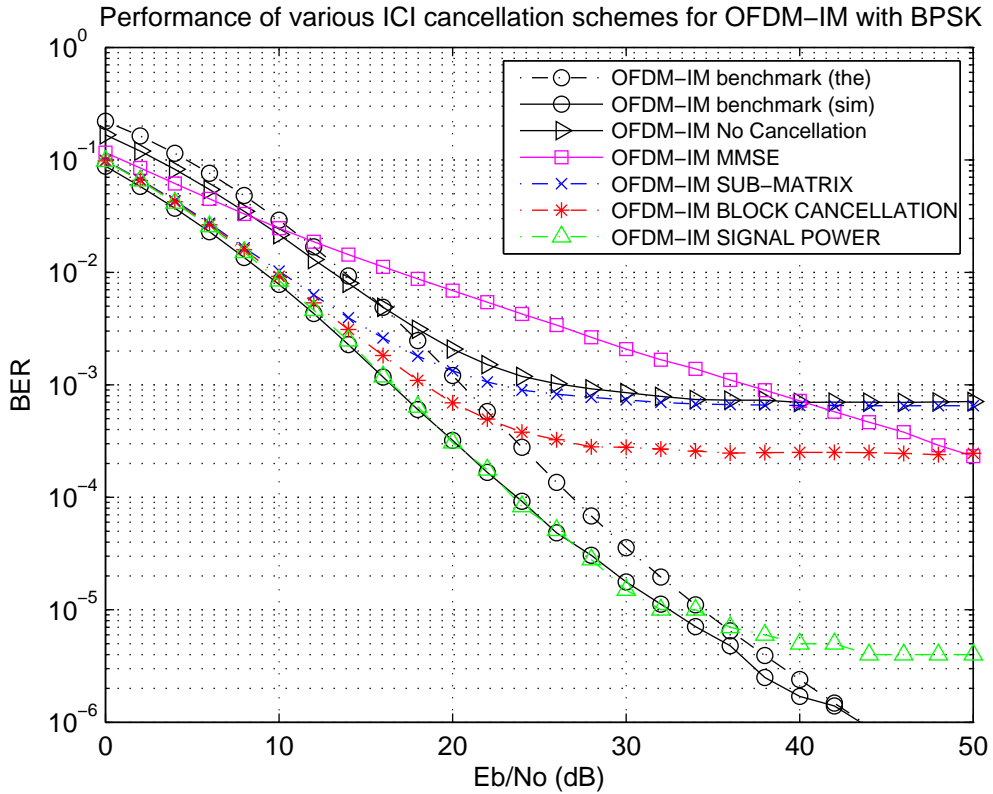


Figure 5.10: Performance of various ICI cancellation schemes of OFDM-IM at 100km/h.

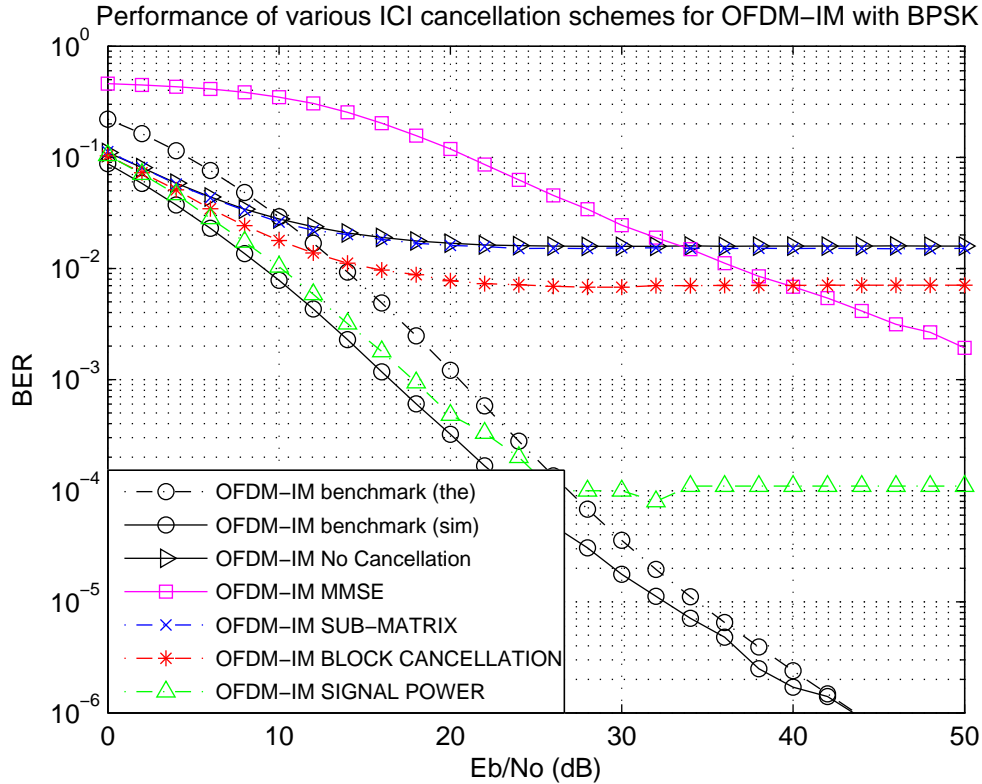


Figure 5.11: Performance of various ICI cancellation schemes of OFDM-IM at 300 km/h.

5.5 Performance of ISK techniques in the presence of ICI

In this section, we examine the effects of ICI on OFDM-GISK compared to classical OFDM. Figure 5.12 shows how the various configurations of $N = 8$ GISK perform in a dispersive channel. As it can be observed, only OFDM-ISK with $N = 8$ outperforms the classical OFDM. Furthermore, as we increase the data rate i.e. the number of sub-carriers used, the resistance to ICI decreases. In contrast, when using $N = 16$ sub-carriers, OFDM-ISK as well as GISK with $n = 2$ gives a lower error floor than OFDM as illustrated in Figure 5.13. As shown before

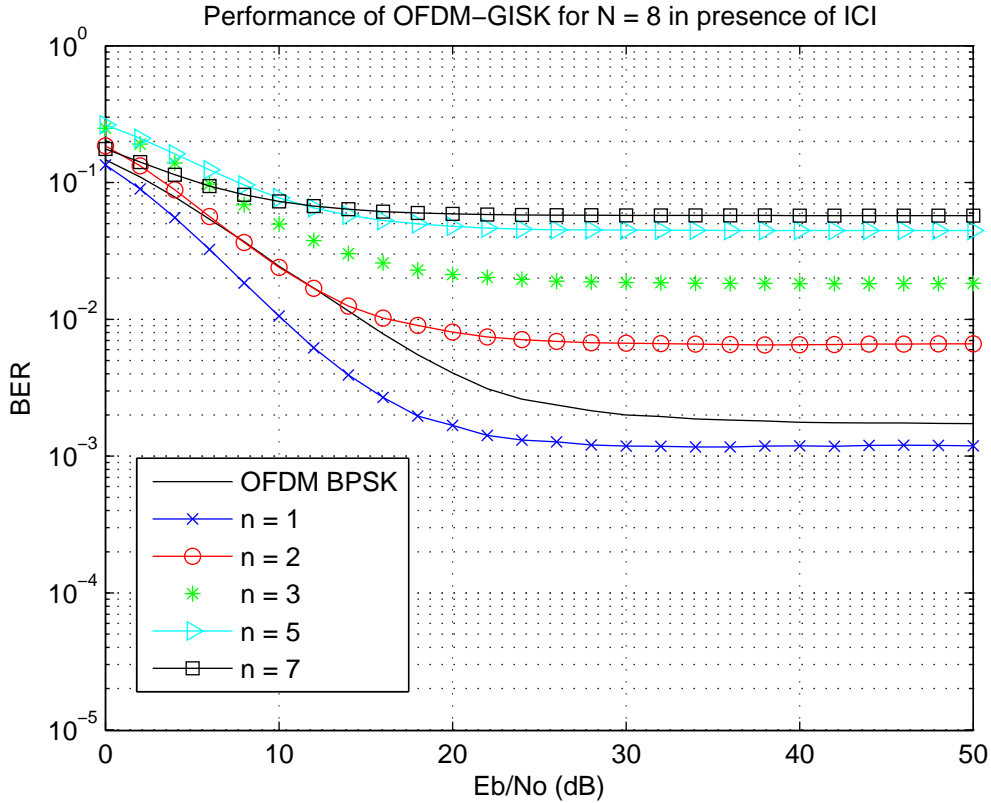


Figure 5.12: Performance of OFDM-GISK for $N = 8$ at 100 km/h.

in Section 4.4, as we increase the number of sub-carriers, increasing n improves SE at a cost of BER. In general, we can say that although OFDM-GISK configurations perform better with lower N values, higher values of N are less susceptible to ICI. This makes sense as for example, $N = 8$ $n = 2$ scheme will have six '0' sub-carriers whereas an $N = 16$ $n = 2$ scheme will have fourteen '0' sub-carriers. In addition, improving the SE will make the system more vulnerable to ICI.

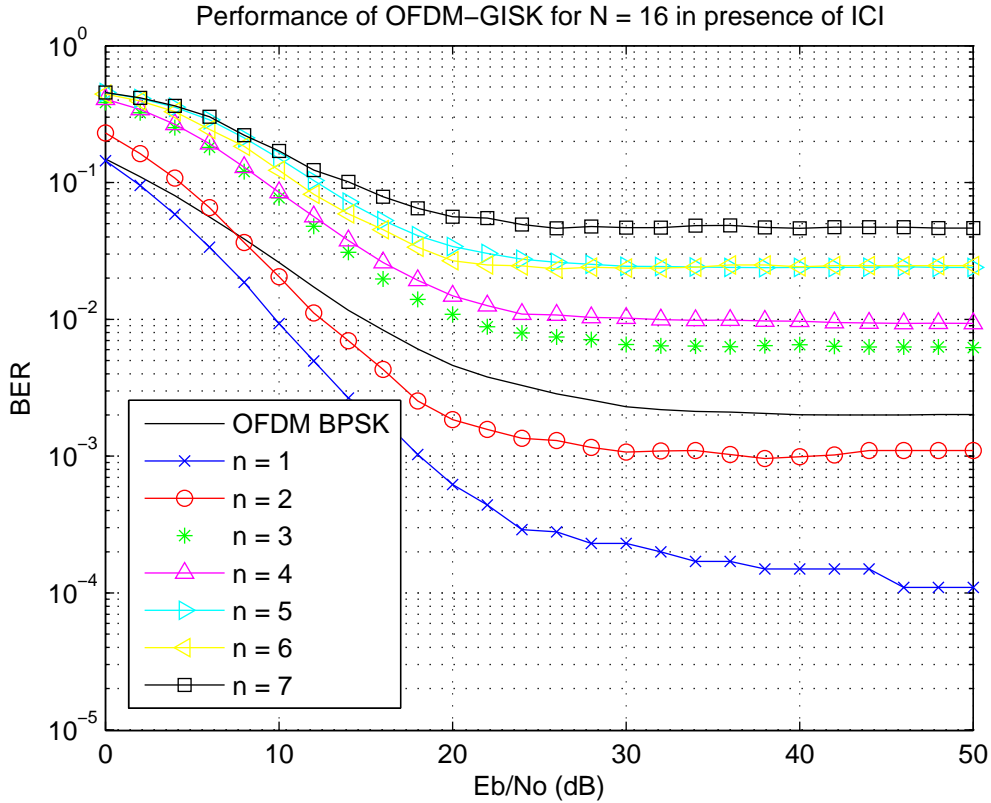


Figure 5.13: Performance of OFDM-GISK for $N = 16$ at 100 km/h.

5.6 Summary

In this chapter, we examined the performance of the OFDM-IM technique in NBI, proposed a mitigation method based on compressive sensing and evaluated the effects of ICI on our newly designed GISK modulation. It was shown that compared to classical OFDM, OFDM-IM is quite resilient to NBI interference for up to SNIR's of -15dB. For very high interference powers, the CS based approach to NBI cancellation works very well and achieves an error floor at high SNR's of 25dB; this result is good enough for wireless networks. In the presence of ICI, OFDM-GISK performs better with less number of active subcarriers n . As we increase n , the performance degradation is higher compared to classical OFDM.

CHAPTER 6

CONCLUSION

6.1 Conclusions

This thesis presented research that came up with new IM techniques based on sub-carrier index switching and evaluated the performance of IM in the presence of ICI and NBI. In the first part, two new techniques called OFDM-GISK and OFDM-ISK belonging to the family of the so called ISK were designed. The performance analysis was carried out and the analytical and simulation results were compared with previous techniques. It was shown that OFDM-GISK performs better than OFDM and OFDM-IM for most configurations. For example, $N = 8$ $n = 3$ and $n = 3$ OFDM-GISK gave better performance than OFDM-IM at a BER of 10^{-4} . Furthermore, OFDM-ISK method was the highest performing one but spectrally inefficient.

In the second part, the performance of OFDM-IM and ISK based schemes were studied under the effects of two different types of interference, NBI and ICI. It

was shown that in contrast to OFDM, OFDM-IM, generally performed better under NBI. In the case of OFDM, the degradation was basically dependent on the SNIR whereas increasing the number of jammers induced a slight change in the performance of OFDM-IM. A previously designed mitigation technique based on CS was modified and adopted to cancel the effects of NBI. It was shown that the method worked for even very high interference powers.

Lastly, It was shown that OFDM-GISK techniques are more resilient to ICI than classical OFDM for a low number of active sub-carriers. Although systems with less total sub-carriers give a better BER performance, higher N systems with low values of n are more resilient to ICI. OFDM-ISK performed better than OFDM and OFDM-IM in the presence of ICI.

In summary the main results are:

- Design of new trans-receive schemes based on IM.
- Analysis and simulation of the performance of the new schemes.
- Investigating the susceptibility of IM techniques to NBI compared to classical OFDM systems.
- Studying the impact of ICI on the new proposed modulation schemes compared to OFDM by simulations.

6.2 Future Research

The newly designed schemes have been designed for SISO systems. The next step is to implement them on MIMO media and combine them with the SSK to form the so called Space Frequency Keying (SFK). Furthermore, as we move to large scale MIMO systems, ML based receivers will not be suitable for such applications. Therefore, there is a need to design lower complexity receivers based on concepts such as spectrum sensing. Lastly, the analysis so far has been done for Rayleigh fading channels with perfect CSI (imperfect CSI in the case of IM), so the performance of such schemes should be analyzed for different fading environments such as the Rician or Nakagami models.

In terms of the study done on ICI and NBI, there is a need to design low complexity detectors for the cases of ISK techniques. Despite the fact that OFDM-IM proved to be quite resilient to NBI, mitigation schemes can still be designed to enhance the performance further. Last but not least, a more practical direction can be taken to implement these techniques whether on software defined radio or on hardware using digital technologies with rapid processing power such as FPGA boards.

REFERENCES

- [1] E. Basar, U. Aygolu, E. Panayirci, and H. V. Poor, “Orthogonal frequency division multiplexing with index modulation,” *2012 IEEE Global Communications Conference (GLOBECOM)*, vol. 61, no. 22, pp. 4741–4746, 2012.
- [2] L. Hanzo, Y. Akhtman, and L. Wang, *MIMO-OFDM for LTE, Wi-Fi and WiMAX*. John Wiley and Sons, 2011.
- [3] R. Mesleh, H. Haas, A. Chang Wook, and Y. Sangboh, “Spatial Modulation - A New Low Complexity Spectral Efficiency Enhancing Technique,” *Communications and Networking in China, 2006. ChinaCom '06. First International Conference on*, pp. 1–5, 2006.
- [4] J. Jeganathan, A. Ghayeb, L. Szczecinski, and A. Ceron, “Space shift keying modulation for MIMO channels,” *IEEE Transactions on Wireless Communications*, vol. 8, no. 7, pp. 3692–3703, 2009.
- [5] N. LaSorte, W. J. Barnes, and H. H. Refai, “The History of Orthogonal Frequency Division Multiplexing,” in *IEEE GLOBECOM 2008 - 2008 IEEE Global Telecommunications Conference*. IEEE, 2008, pp. 1–5.

- [6] S. Weinstein, “The history of orthogonal frequency-division multiplexing [History of Communications,” *IEEE Communications Magazine*, vol. 47, no. 11, pp. 26–35, nov 2009.
- [7] Miowen Wen, X. Cheng, and L. Yang, “Optimizing the Energy Efficiency of OFDM with Index Modulation,” in *IEEE International Conference on Communication Systems (ICCS), 2014*, 2014, pp. 31–35.
- [8] E. Basar, Ü. Aygözü, and E. Panayirci, “Orthogonal Frequency Division Multiplexing with Index Modulation,” in *First International Black Sea Conference on Communications and Networking (BlackSeaCom), 2013*, 2013, pp. 1–32.
- [9] T. Datta, H. S. Eshwarajah, A. Chockalingam, and S. Member, “Generalized Space and Frequency Index Modulation,” *IEEE Transactions on Vehicular Technology*, vol. PP, no. 99, pp. 1–14, 2015.
- [10] T. Sanjana and M. N. Suma, “Comparison of NBI suppression methods in OFDM systems,” *International Journal of Science, Engineering and Technology Research (IJSETR)*, vol. 3, no. 3, pp. 470–477, 2014.
- [11] C. G. K. Yong Soo Cho, Jaekwon Kim, Won Young Yang, *MIMO-OFDM Wireless Communications with MATLAB*, 2010, no. 1.
- [12] B. Lathi and Z. Ding, *Modern Digital and Analog Communication Systems*, 4th ed. Oxford University Press, 2010.

- [13] B. Muquet, Z. Wang, S. Member, G. B. Giannakis, M. D. Courville, and P. Duhamel, “Cyclic Prefixing or Zero Padding for Wireless Multicarrier Transmissions ?” *IEEE Transactions on Communications*, vol. 50, no. 12, pp. 2136–2148, 2002.
- [14] M. S. Sohail, T. Y. Al-naffouri, and S. N. Al-ghadhban, “Narrow band interference cancelation in OFDM: A structured maximum likelihood approach,” in *2012 IEEE 13th International Workshop on Signal Processing Advances in Wireless Communications (SPAWC)*, no. 1, 2012, pp. 45–49.
- [15] A. Ali, M. Masood, M. S. Sohail, S. Al-Ghadhban, and T. Y. Al-Naffouri, “Narrowband Interference Mitigation in SC-FDMA Using Bayesian Sparse Recovery,” in *2015 IEEE International Conference on Communications (ICC)*, 2014, pp. 1–14. [Online]. Available: <http://arxiv.org/abs/1412.6137>
- [16] A. Gomaa, K. M. Z. Islam, and N. Al-dhahir, “Two Novel Compressed-Sensing Algorithms for NBI Detection in OFDM Systems,” in *2010 IEEE International Conference on Acoustics, Speech and Signal Processing*, no. 7, 2010, pp. 3294–3297.
- [17] A. Gomaa and N. Al-dhahir, “A Compressive Sensing Approach to NBI Cancellation in Mobile OFDM Systems,” in *IEEE Global Telecommunications Conference (GLOBECOM 2010)*, no. 1, pp. 1–5.
- [18] —, “Compressive-Sensing-Based Approach for NBI Cancellation in MIMO-OFDM,” in *2011 IEEE Global Telecommunications Conference (GLOBE-*

COM 2011), no. 3, pp. 1 – 5.

- [19] —, “A Sparsity-Aware Approach for NBI Estimation in MIMO-OFDM,” *IEEE TRANSACTIONS ON WIRELESS COMMUNICATIONS*, vol. 10, no. 6, pp. 1854–1862, 2011.
- [20] J. Mietzner, R. Schober, L. Lampe, W. Gerstacker, and P. Hoeher, “Multiple-antenna techniques for wireless communications - a comprehensive literature survey,” *IEEE Communications Surveys & Tutorials*, vol. 11, no. 2, pp. 87–105, 2009.
- [21] M. Di Renzo, H. Haas, A. Ghayeb, S. Sugiura, and L. Hanzo, “Spatial Modulation for Generalized MIMO: Challenges, Opportunities, and Implementation,” *Proceedings of the IEEE*, vol. 102, no. 1, pp. 56–103, 2014.
- [22] R. Mesleh, S. Engelken, S. Sinanovic, and H. Haas, “Analytical SER Calculation of Spatial Modulation,” in *IEEE 10th International Symposium on Spread Spectrum Techniques and Applications, 2008*, 2008, pp. 272–276.
- [23] E. Basar, U. Aygolu, E. Panayirci, and H. V. Poor, “Performance of Spatial Modulation in the Presence of Channel Estimation Errors,” *IEEE Communications Letters*, vol. 16, no. 2, pp. 176–179, 2012.
- [24] R. Mesleh and S. S. Ikki, “On the effect of Gaussian imperfect channel estimations on the performance of space modulation techniques,” *IEEE Vehicular Technology Conference*, 2012.

- [25] —, “A High Spectral Efficiency Spatial Modulation Technique,” in *IEEE 80th Vehicular Technology Conference (VTC Fall)*, 2014, pp. 1–5.
- [26] R. Mesleh, S. S. Ikki, and H. M. Aggoune, “Quadrature Spatial Modulation,” *IEEE Transactions on Vehicular Technology*, vol. 64, no. 6, pp. 2738 – 2742, 2014.
- [27] J. Jeganathan, A. Ghayeb, and L. Szczecinski, “Generalized Space Shift Keying Modulation for MIMO Channels,” in *2008 IEEE 19th International Symposium on Personal, Indoor and Mobile Radio Communications*, 2008.
- [28] R. R. Gutierrez, L. Zhang, and J. Elmirghani, “Generalized Phase Spatial Shift Keying Modulation for MIMO Channels,” *Electrical engineering and electronics*, pp. 1–5, 2011.
- [29] M. Di Renzo and H. Haas, “On the performance of space shift keying MIMO systems over correlated Rician fading channels,” *2010 International ITG Workshop on Smart Antennas, WSA 2010*, no. Wsa, pp. 72–79, 2010.
- [30] —, “Space shift keying (SSK) modulation with partial channel state information: Optimal detector and performance analysis over fading channels,” *IEEE Transactions on Communications*, vol. 58, no. 11, pp. 3196–3210, 2010.
- [31] R. Mesleh, H. Haas, C. Ahn, and S. Yun, “Spatial modulation-OFDM,” in *Proc. of the International OFDM Workshop*, 2006, pp. 30–34.

- [32] S. Ganesan and R. Y. Mesleh, “On the performance of spatial modulation OFDM,” in *Asilomar Conference on Signals, Systems and Computers (ACSSC)*, 2006, pp. 1825–1829.
- [33] R. Mesleh, S. Ganesan, and H. Haas, “Impact of Channel Imperfections on Spatial Modulation OFDM,” in *2007 IEEE 18th International Symposium on Personal, Indoor and Mobile Radio Communications*, 2007, pp. 1–5.
- [34] R. Abu-alhiga and H. Haas, “Subcarrier-index modulation OFDM,” *IEEE International Symposium on Personal, Indoor and Mobile Radio Communications, PIMRC*, vol. 1, pp. 177–181, 2009.
- [35] D. Tsonev, S. Sinanovic, and H. Haas, “Enhanced subcarrier index modulation (SIM) OFDM,” *2011 IEEE GLOBECOM Workshops, GC Wkshps 2011*, pp. 728–732, 2011.
- [36] E. Baar, “Multiple-Input Multiple-Output OFDM with Index Modulation,” *IEEE Signal Processing Letters*, vol. 22, no. 12, pp. 2259–2263, 2015.
- [37] S. Wangl, B. Xul, H. Bal, Y. Xiaol, and L. Danl, “MIMO-OFDM with interleaved subcarrier-index modulation,” in *10th International Conference on Wireless Communications, Networking and Mobile Computing (WiCOM 2014)*, no. M1, 2014, pp. 35–37.
- [38] R. Fan, Y. J. Yu, and Y. L. Guan, “Orthogonal frequency division multiplexing with generalized index modulation,” *Global Communications Conference (GLOBECOM), 2014 IEEE*, vol. 3, no. 1, pp. 3880–3885, 2014.

- [39] X. Yang, Z. Zhang, P. Fu, and J. Zhang, "Spectrum-Efficient Index Modulation with Improved Constellation Mapping," in *International Workshop on High Mobility Wireless Communications (HMWC), 2015*, 2015, pp. 91–95.
- [40] R. Fan, Y. J. Yu, and Y. L. Guan, "Generalization of Orthogonal Frequency Division Multiplexing With Index Modulation," *IEEE Transactions on Wireless Communications*, vol. 14, no. 10, pp. 5350–5359, 2015.
- [41] A. I. Siddiq, "Low Complexity OFDM-IM Detector by Encoding All Possible Subcarrier Activation Patterns," *IEEE Communications Letters*, vol. 20, no. 3, pp. 446–449, 2016.
- [42] Y. Xiao, S. Wang, L. Dan, X. Lei, P. Yang, and W. Xiang, "OFDM With Interleaved Subcarrier-Index Modulation," *IEEE Communications Letters*, vol. 18, no. 8, pp. 1447–1450, 2014.
- [43] X. Cheng, M. Wen, L. Yang, and Y. Li, "Index modulated OFDM with interleaved grouping for V2X communications," *17th International IEEE Conference on Intelligent Transportation Systems (ITSC)*, pp. 1097–1104, 2014.
- [44] E. Basar, "OFDM with Index Modulation Using Coordinate Interleaving," *IEEE Wireless Communications Letters*, vol. 2337, no. c, pp. 1–1, 2015.
- [45] M. Zhang, H. Wang, X. Cheng, L.-q. Yang, and X. Zhou, "Quadrature Index Modulated OFDM with Interleaved Grouping for V2X Communications," in *International Conference on Computing, Networking and Communications (ICNC), 2016*, 2016, pp. 1–5.

- [46] B. Zheng, F. Chen, M. Wen, F. Ji, H. Yu, and Y. Liu, “Low-Complexity ML Detector and Performance Analysis for OFDM With In-Phase/Quadrature Index Modulation,” *IEEE Communications Letters*, vol. 19, no. 11, pp. 1893–1896, 2015.
- [47] Y. Ko, “A Tight Upper Bound on Bit Error Rate of Joint OFDM and Multi-Carrier Index Keying,” *IEEE Communications Letters*, vol. 18, no. 10, pp. 1763–1766, 2014.
- [48] M. Wen, X. Cheng, M. Ma, B. Jiao, and H. V. Poor, “On the Achievable Rate of OFDM With Index Modulation,” *IEEE Transactions on Signal Processing*, vol. 64, no. 8, pp. 1919–1932, 2016.
- [49] E. Engineering, “Optical OFDM with Index Modulation for Visible Light Communications,” in *4th International Workshop on Optical Wireless Communications (IWOW), 2015*, 2015, pp. 11–15.
- [50] H. Elgala and T. D. C. Little, “SEE-OFDM : Spectral and Energy Efficient OFDM for Optical IM / DD Systems,” in *IEEE 25th Annual International Symposium on Personal, Indoor, and Mobile Radio Communication (PIMRC), 2014*, 2014, pp. 851–855.
- [51] H. Jafarkhani, *Space-Time Coding, Theory And Practice*. Cambridge University Press, 2006.
- [52] M. Chiani and D. Dardari, “Improved exponential bounds and approximation for the Q-function with application to average error probability compu-

- tation,” in *Global Telecommunications Conference, 2002. GLOBECOM '02. IEEE*, vol. 2. IEEE, 2002, pp. 1399–1402.
- [53] J. Jeganathan, A. Ghrayeb, and L. Szczecinski, “Spatial modulation: optimal detection and performance analysis,” *IEEE Communications Letters*, vol. 12, no. 8, pp. 545–547, 2008.
- [54] R. A. Horn and C. R. Johnson, *Matrix Analysis*, 1985.
- [55] R. Gallager, “Circularly-symmetric Gaussian random vectors,” *Preprint*, pp. 1–9, 2008. [Online]. Available: <http://www.rle.mit.edu/rgallager/documents/CircSymGauss.pdf>
- [56] M. Elia and G. Taricco, “Integration of the exponential function of a complex quadratic form,” *Applied Mathematics E - Notes*, vol. 3, pp. 95–98, 2003.
- [57] A. Batra and J. R. . Zeidler, “Narrowband Interference Mitigation in BICM OFDM Systems,” in *2009 IEEE International Conference on Acoustics, Speech and Signal Processing*, 2009, pp. 2605–2608.
- [58] C.-H. Wu, W.-H. Chung, and H.-W. Liang, “OMP-based detector design for space shift keying in large MIMO systems,” *2014 IEEE Global Communications Conference*, no. M1, pp. 4072–4076, 2014.
- [59] S. Boyd and L. Vandenberghe, *Convex Optimization*, 7th ed. Cambridge University Press, 2004.

- [60] E. J. Candes and T. Tao, “Decoding by Linear Programming,” *IEEE Transactions on Information Theory*, vol. 51, no. 12, pp. 4203–4215, 2005.
- [61] E. Candes and T. Tao, “Decoding by Linear Programming,” vol. 40698, no. December, pp. 1–22, 2004.
- [62] Z. Han, H. Li, and W. Yin, *Compressive Sensing for Wireless Networks*, 2013.
- [63] M. Grant and S. Boyd, “Graph implementations for nonsmooth convex programs,” in *Recent Advances in Learning and Control*, ser. Lecture Notes in Control and Information Sciences, V. Blondel, S. Boyd, and H. Kimura, Eds. Springer-Verlag Limited, 2008, pp. 95–110.
- [64] I. CVX Research, “{CVX}: Matlab Software for Disciplined Convex Programming, version 2.0,” [\url{http://cvxr.com/cvx}](http://cvxr.com/cvx), aug 2012.
- [65] J. G. Proakis and M. Salehi, *Digital Communications*, 5th ed. McGraw-Hill, 2008.
- [66] L. L. Hanzo, M. Münster, B. J. Choi, and T. Keller, *OFDM and MC-CDMA for broadband multi-user communications, WLANs, and broadcasting*. J. Wiley, 2003.

Vitae

- Name: Mohammad Umair Yaqub
- Nationality: Pakistan
- Date of Birth: 30/05/1992
- Email: *umairy@kfupm.edu.sa*
- Permanent Address: Riyadh Street, Rabee Terraces, KFUPM, Dhahran, Kingdom of Saudi Arabia
- Bachelor of Science in Electrical Engineering, King Fahd University of Petroleum and Minerals, January, 2013.
- Joined King Fahd University of Petroleum and Minerals as a Research Assistant, September, 2013.
- Master of Science in Telecommunication Engineering, King Fahd University of Petroleum and Minerals, September, 2016.

PUBLICATIONS

- M. Yaqub and M. Al-Ahmadi, "Application of Combined Arma-Neural Network Models to Predict Stock Prices", in Proceedings of *The 3rd Multidisciplinary International Social Networks Conference on Social Informatics* (Data Science, 2016). DOI: <http://dx.doi.org/10.1145/2955129.2955171>

- M. Yaqub and S. Al-Ghadhban, "OFDM with generalized index shift keying", submitted to the *9th IEEE-GCC Conference and Exhibition 2017 (9th IEEE-GCC 2017)*.